TALLINN UNIVERSITY OF TECHNOLOGY
SCHOOL OF ENGINEERING
Department of Materials and Environmental Technology

OIL SHALE ASH BASED PCC PRODUCTION: EFFECT OF OPERATING PARAMETERS AND ADDITIVES ON PCC PRECIPITATION EFFICIENCY AND QUALITY

PÕLEVKIVITUHAST SADESTATUD KALTSIUMKARBONAADI TOOTMISE TÖÖPARAMEETRITE JA LISANDITE MÕJU UURING.

MASTER'S THESIS

Student: Fatima Precious Otori

Student code: 195457KAYM

Supervisors: Kadriann Tamm, Research Scientist, PhD

Mai Uibu, Senior Research Scientist, PhD

Tallinn 2021

AUTHOR'S DECLARATION

Hereby I declare, that I have written this thesis independently.
No academic degree has been applied for based on this material. All works, major viewpoints and data of the other authors used in this thesis have been referenced.

"" .....05..... 2021…..

Author: .....
/signature /

Thesis is in accordance with terms and requirements

"....." ..... 21….

Supervisor: ….....
/signature/

Accepted for defence

".....".....21… .

Chairman of theses defence commission: .....
/name and signature/

Non-exclusive licence for reproduction and publication of a graduation thesis[1]

I, Fatima Precious Otori,

1. grant Tallinn University of Technology free licence (non-exclusive licence) for my thesis Oil shale ash based PCC production: effect of operating parameters and additives on PCC precipitation efficiency and quality,

supervised by Kadriann Tamm and Mai Uibu

1.1 to be reproduced for the purposes of preservation and electronic publication of the graduation thesis, incl. to be entered in the digital collection of the library of Tallinn University of Technology until expiry of the term of copyright;

1.2 to be published via the web of Tallinn University of Technology, incl. to be entered in the digital collection of the library of Tallinn University of Technology until expiry of the term of copyright.

2. I am aware that the author also retains the rights specified in clause 1 of the non-exclusive licence.

3. I confirm that granting the non-exclusive licence does not infringe other persons' intellectual property rights, the rights arising from the Personal Data Protection Act or rights arising from other legislation.

18.05.2021

[1] *The non-exclusive licence is not valid during the validity of access restriction indicated in the student's application for restriction on access to the graduation thesis that has been signed by the school's dean, except in case of the university's right to reproduce the thesis for preservation purposes only. If a graduation thesis is based on the joint creative activity of two or more persons and the co-author(s) has/have not granted, by the set deadline, the student defending his/her graduation thesis consent to reproduce and publish the graduation thesis in compliance with clauses 1.1 and 1.2 of the non-exclusive licence, the non-exclusive license shall not be valid for the period.*

Department of Materials and Environmental Technology

THESIS TASK

Student: Fatima Precious Otori, 195457KAYM

Study programme, Material and Processes of Sustinable Energetics

main speciality: Materials for Sustinable Energetics

Supervisor(s): Kadriann Tamm, Research Scientist, PhD, 51925707

Mai Uibu, Senior Research Scientist, PhD, 5214319

Thesis topic:

(in English): Oil shale ash based PCC production: effect of operating parameters and additives on PCC precipitation efficiency and quality.

(in Estonian): Põlevkivituhast sadestatud kaltsium karbonaadi tootmise tööparameetrite ja lisandite mõju uuring.

Thesis main objectives:

1. Study of leaching and dissolution behaviour of Ca^{2+} in a ash-NH_4COOCH_3 system.
2. To study the carbonation process and the absorption of CO_2 by Ca^{2+} and SO_4^{2-} alkaline rich leachates.
1. To study the precipitation, morphology and PSD of $CaCO_3$ under the influence of $NaHCO_3$ as an additive.

Thesis tasks and time schedule:

No	Task description	Deadline
1.	Study of research procedures and materials	1st sem
2.	Literature review	2nd sem 3rd sem
3.	Experimental procedure	4th sem
4.	Thesis finaliztaion	4th sem

Language: English **Deadline for submission of thesis:** "...21..."...May.....2021….a

Student: Fatima P. Otori ..... "....."…….....2021….a

/signature/

Supervisor: Kadriann Tamm …….. "....."....2021….a

/signature/

Supervisor: Mai Uibu …..... "....."....2021….a

/signature/

Head of study programme: Sergei Bereznev ....."....."....2021.a

/signature/

TABLE OF CONTENTS

Table of Contents

PREFACE

This work was partly completed within the framework of LEP19098 "Applied research on the possibilities of oil shale ash valorisation and recycling" financed by R-S OSA Service OÜ.

The topic of this thesis was proposed by Mai Uibu (Senior Research Scientist, PhD) and supervised by Kadriann Tamm (Research Scientist, PhD).

The experimental work was carried out in the Laboratory of Inorganic Materials at the department of Materials and Environmental Technology and at the University of Tartu, Department of Geology where the produced product characterization analyses were carried out. Assistance in experimental set up was provided by Ae Leier.

I would like to express my profound gratitude to my very supportive and responsive supervisor Kadriann Tamm, and my co-supervisor Mai Uibu for her guidance and encouragement. I would also like to specially thank Can Rüstü Yörük and Ae Leier for their assistance and training in carrying out my sample analysis. I am also extending my thanks to the whole Laboratory of Inorganic Material team and the team from the University of Tartu, Department of Geology where some of the analyses were carried out.

Finally, I would like to thank and appreciate my family and loved ones for their unwavering support and encouragement.

The aim of this work was focused on how to produce high quality precipitated calcium carbonate (PCC) for commercial purposes using oil shale ash and ammonium salt solution as the core materials. The study of the leaching and precipitation behavior of $CaCO_3$ was carried out in an ash-NH_4COOCH_3 – CO2 containing gas system under different operating parameters like temperature, residence time, agitation, bubble size, and additives. To ensure the quality of the product, the experiments were performed for comparison with addition of $NaHCO_3$ to the solution to enhance the precipitation procedure and quality of PCC produced.

Keywords: PCC, oil shale ash, ammonium solvent, $NaHCO_3$ addition, Carbonization

Tallinn, May 21st, 2021

Fatima Precious Otori

LIST OF FIGURES

LIST OF TABLES

LIST OF ABBREVIATIONS

CAGR – Compound annual growth rate

CMCS - Carboxylmethyl chitosan

CTAB - Cetyl trimethylammonium bromide

DDS - Dodecyl sulfonate

DDTAB - Dodecyltrimethylammonium bromide

EC – Electrical conductivity

EDTA - Ethylenediaminetetraacetic acid

FA – Fly Ash

GCC – Ground calcium carbonate

GEN - General

OSA – Oil shale ash

PAA – Poly acrylic acid

PCC – Precipitated calcium carbonate

PDDA – Polydiallyldmethylammonium chloride

PSD – Particle size distribution

PVC – Poly vinyl chloride

SEM – Scanning electron microscope

SDBS - Sodium dodecyl benzenesulfonate

SDS - Sodium dodecyl sulfate

SSA – Specific surface area

INTRODUCTION

Over 90% of the Estonian basic power supply generated from oil shale – fired thermal power plants. From recent reports in 2020, about 6.4 million tons of oil shale is fired. The challenging problem today is the handling of oil shale ashes, although the amount of these ashes has reduced considerably, as the share of oil shale-based energetics diminishes. About2.9 million tons of these ashes were produced in 2020, compared to the report of 2016 which reported 7.0 million tons [1]. Currently this is mostly disposed on ash fields, which poses a threat to surface and groundwater [2]. In addition, during the incineration stage of oil shale, greenhouse gases (CO_2) are released into the atmosphere, which contributes to the climate change crises being faced today. To significantly reduce the carbon footprint of the Estonian energy production, the means for capturing and storing the CO_2 released during the burning process should be adopted.

The oil shale ash (OSA) is not considered toxic waste because it meets the safety requirements of the Estonian law. The ash can be used for various purposes, but the share of ash recycling is still very low. Examples of ash utilization [2]:

i. It can be applied as a fertilizer during farming.
ii. Due to its alkaline nature, it can be applied to the soil to reduce soil acidity.
iii. It can be used as a filler in road constructions.
iv. It can be used in brick making.
v. It can be used as a replacement of limestone in PCC production.

Forming OSA shows significant economic potential in various sectors but current study focuses on the production of precipitated calcium carbonate (PCC). PCC is used in a wide variety of products, such as adhesives, sealants, food and pharmaceuticals, paints, coatings, paper, cements, and construction materials. Conventional production of PCC includes the mining of natural limestone in quarries and using large amounts of fossil fuels for limestone thermal decomposition which produces excessive hazardous emissions.

Recently, some innovative solutions have been studied in the production of PCC based on Ca-rich wastes/by-products such as steel slag or OSA. During the incineration stage of oil shale, the CO_2 produced could be captured and stored to use it as a reactant during the production of PCC. This in turn reduces the carbon footprint [3].

Therefore, the utilization of OSA could bring about environmental economic and social benefit. The environmental benefits of OSA utilization in the construction industry, PCC

production etc. would reduce the amounts of OSA deposited in landfills, the depletion of natural resources (limestone) and the emission of greenhouse gases. The use of OSA could also lead to some positive social impacts by providing jobs for the people involved in projects concerning OSA and contributing by that to Estonian Green Turn [4].

1. LITERATURE REVIEW

1.1 Precipitated Calcium Carbonate

Precipitated Calcium Carbonate (PCC) is a synthetic, purified, fine white powder without odour or taste and it is considered non-toxic. PCC can be derived from oil shale ash due to its high calcium content and from other calcium rich wastes which could be considered as a replacement of limestone [5]. It is a refined form of $CaCO_3$ used in various industrial applications, PCC have been commercially produced since 1841. The pioneer producer was the English company John E. Sturge Ltd., which treated the residual calcium chloride from their potassium chlorate manufacture with soda ash and carbon dioxide [6]. This precipitation occurs under defined conditions. The form of precipitated calcium carbonate obtained – in other words, its particle shape and particle size distribution – depends on the precipitation conditions, such as concentration, temperature and temperature change during precipitation, agitation energy, pH, and other factors.

The different shapes allow the PCC to act as a very important additive in paper, adhesives, plastics, rubber, inks, pharmaceuticals, nutritional supplements, and many other demanding applications.

Naturally, the most common source of $CaCO_3$ is found in a sedimentary rock called limestone, which contains mainly $CaCO_3$ and some magnesium carbonate ($MgCO_3$) as well as other elements as impurities. This limestone can be found almost everywhere on earth. When it is mined, majority of it is used in the construction industries. In some cases, if the purity and morphology of the natural limestone is sufficient, then after grinding, it can be used in other industries like the pulp and paper industry. This $CaCO_3$ gotten from limestone by grinding is known as Ground Calcium Carbonate (GCC) [7].

On the other hand, when $CaCO_3$ is produced synthetically in a precipitation process it is referred to Precipitated Calcium Carbonate (PCC). From studies, the quality of the PCC compared to the GCC is generally higher as the conditions under which it is produced can be adjusted to give the desired properties ranging from brightness to crystal shape and size [7].

Hence, since the size and shape of PCC can be controlled during the production stage, it is used more in advanced applications than the GCC. The common differences seen between PCC and GCC is illustrated in the table 1.

Table 1 Common differences between PCC and GCC [8]

	PCC	GCC
Powder characteristics	Regular shape and size usually between 1 – 3 µm	Irregular shape and size usually between 5 – 10 µm
Brightness	94 - 99%	89 - 93%
True Density in plastics	Weighs less (2.4 - 2.6 g/cm^3)	Weighs more (2.6 - 2.9 g/cm^3)
Modification functions	Better impact strength and rigidity	Better tensile strength

Table 2 The typical shapes of calcium carbonate ($CaCO_3$) particles viewed using SEM. [9]

Shapes	**Cubic**	**Rod**	**Sphere**	**Flower**
Images	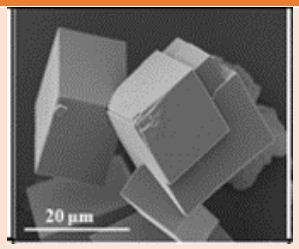	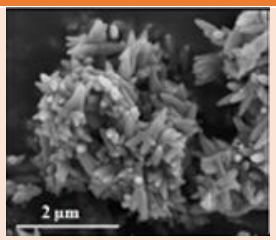	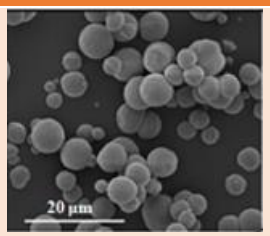	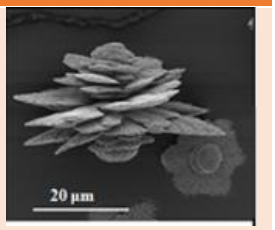
Average Diameter	2.0 – 20 µm	2.1 – 3 µm	0.2 – 5.0 µm	20 – 100 µm
Crystalline Phase	Calcite (β-$CaCO_3$)	Aragonite (λ-$CaCO_3$)	Vaterite (µ-$CaCO_3$)	Vaterite (µ-$CaCO_3$)
Crystalline System	Rhomboedric	Orthorhombic	Hexagonal	Hexagonal

1.2 PCC Production

There are several existing technologies for producing PCC and these methods are [10]:

i. Carbonation process.
ii. Lime-soda process.
iii. Solvay process.

In the production of PCC, the carbonation process is widely used because, PCC is produced as the main product while in the Solvay and lime-soda methods, PCC is usually

a by-product. The calcium rich source can be either limestone or waste materials like steel-making slag or oil shale ash.

1.2.1 Carbonation Process

Of all these methods, the carbonation process is the most widely used method in producing PCC. The reaction equations illustrated below [11]:

$$CaCO_{3(s)} \xrightarrow{Heat} CaO_{(s)} + CO_{2(g)} \quad \Delta H^{1000℃} = 163KJ/mol \tag{0.1}$$

$$CaO_{(s)} + H_2O_{(l)} \rightarrow Ca(OH)_{2(S)} \quad \Delta H^{20℃} = -65KJ/mol \tag{0.2}$$

$$Ca(OH)_{2(s)} + CO_{2(g)} \leftrightarrow CaCO_{3(s)} + H_2O_{(l)} \quad \Delta H^{20℃} = -113KJ/mol \tag{0.3}$$

The first step is crushing the limestone and burning it in a lime kiln at about 1000ºC as illustrated in eq. (1.1). Calcium carbonate from the limestone decomposes into calcium oxide (CaO) (also known as lime or quicklime) and carbon dioxide (CO_2). This reaction is endothermic with a typical energy consumption of 3.5 – 8.0 MJ/kg CaO [12]. The resulting calcium oxide is then mixed with water (known as slaking) to produce calcium hydroxide ($Ca(OH)_2$) (referred to as slaked lime or milk of lime [13]) as is shown in eq. (1.2). The next step is to remove the impurities from the limestone, CO_2 is then bubbled through the solution causing calcium carbon to precipitate as shown in eq. (1.3). Usually, the purified CO_2 from calcination process is re-used in carbonation process [14]. The conditions during the processes can be controlled to produce PCC of the required qualities (i.e., particle size distribution and morphology). The PCC acquired can then be screened and dried or can be delivered in slurry form to the end user depending on the purpose it is required for. One disadvantage of this method is the high energy requirement for burning lime and its significant impact in CO_2 emissions [11]. Therefore, several alternative methods to produce PCC with reduced energy consumption and CO_2 emissions are being considered.

1.2.2 Lime-Soda Process

Another method of producing PCC is through the lime-soda process. In this process, milk of lime is reacted with sodium carbonate (Na_2CO_3) to produce PCC and sodium hydroxide (NaOH) solution. The reaction process is shown in the equation below [16].

$$Ca(OH)_2 + Na_2CO_3 \leftrightarrow CaCO_3 + 2NaOH \quad (0.4)$$

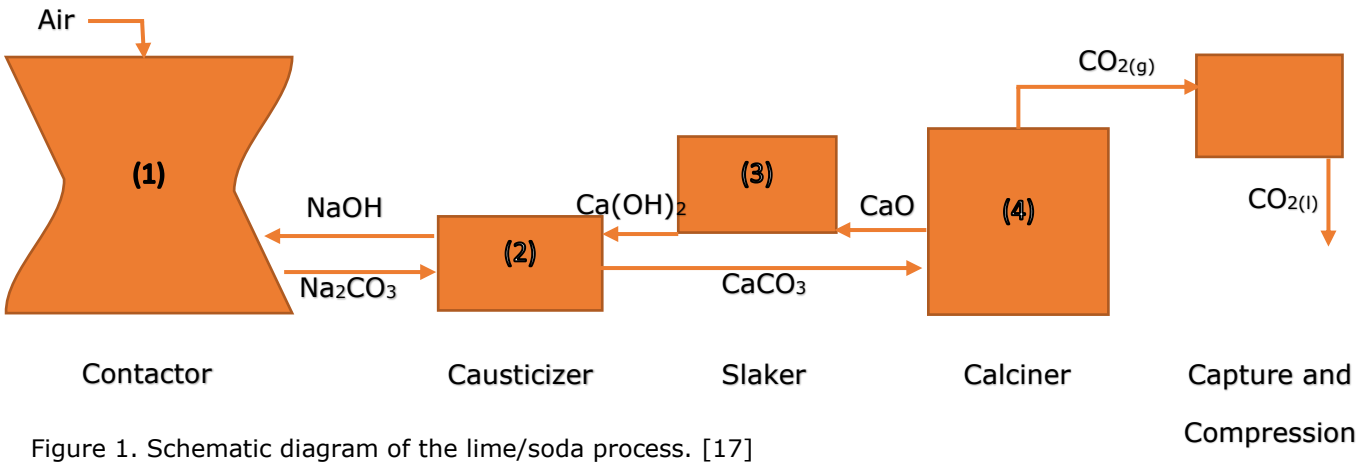

Figure 1. Schematic diagram of the lime/soda process. [17]

The lime-soda process in figure 1 consists of four reaction processes. In the first step, CO_2 was absorbed from air using sodium hydroxide (NaOH) and mixed in the contactor to produce soda (Na_2CO_3). This soda is then reacted with calcium hydroxide ($Ca(OH_2)$) in a reactor called causticizer to reproduce sodium hydroxide which is channeled back to the contactor. This process is the typical lime-soda reaction process. The waste product from this reaction process is the calcium carbonate ($CaCO_3$) which is filtered from the sodium hydroxide solution. To continue the reaction process, the calcium carbonate is converted back to lime (CaO) by heating it up in the calciner, it is then slaked and channeled back to the causticizer for the reaction to be repeated. The CO_2 output from the calciner is usually captured and compressed to reduce its negative emissions [17].

1.2.3 Solvay Process

PCC can also be produced using the Solvay method. In this Solvay process, calcium chloride ($CaCl_2$) is reacted with sodium carbonate (Na_2CO_3) to form calcium carbonate ($CaCO_3$) and sodium chloride (NaCl), shown in the equation below [16].

$$Na_2CO_3 + CaCl_2 \leftrightarrow CaCO_3 + 2NaCl \quad (0.5)$$

This process is known to be the simplest among the three described processes. But for it to be economically viable, it requires a low-cost source of calcium chloride and that is why the process is usually carried out in a satellite facility adjacent to a Solvay process soda ash plant [16].

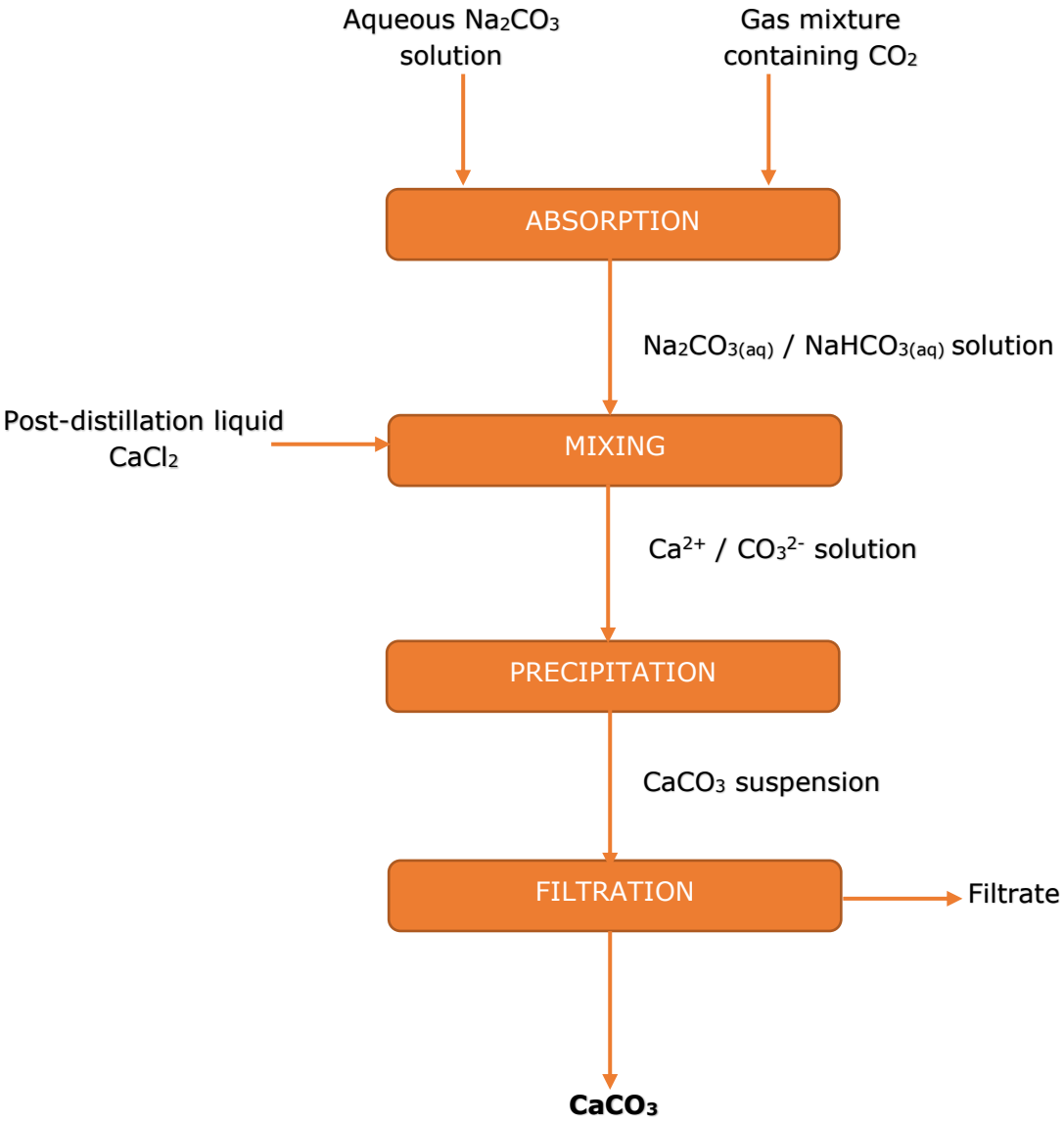

Figure 2 Diagram of the $CaCO_3$ precipitation process using post-distillation liquid from the Solvay process and aqueous Na_2CO_3 solution saturated with CO_2. [18].

The sodium carbonate solution is saturated with CO_2 after which the solution is reacted with calcium chloride solution. The resulting calcium rich solution is precipitated to generate calcium carbonate solution which is then filtered to get the PCC product.

Because of the differences between the three discussed processes, the quality of the PCC produced by each method varies. Each method of producing the PCC gives different impurities present in the PCC. For instance, in the Solvay process, the PCC produced contains chlorine as an impurity, but this chlorine is not found in the PCC produced using other methods. On the other hand, PCC produced using the carbonation and lime-soda methods contain more impurities like $MgCO_3$, Al_2O_3 and Fe_2O_3 which are found in minute amounts in the Solvay process produced PCC. This is because most of the impurities have been removed from the limestone in the earlier stage of reaction. From literature reviews, the typical chemical composition present as impurities in the PCC production processes shown in table 3.

Table 3 Chemical composition/Impurities in PCC by production process (%) [16].

	Carbonation	Lime-soda	Solvay
$CaCO_3$	98.36	98.43	98.62
$CaSO_4$	0.08	0.78	0.63
$MgCO_3$	0.7	0.37	0.21
Al_2O_3	0.09	0.07	0.01
Fe_2O_3	0.07	0.06	0.01
SiO_2	0.1	0.04	0.02
NaCl	-	-	0.1
% H_2O loss	0.6	0.25	0.3
pH (sat. Sol)	9.4	10.3	8.5

1.2.4. Alternative PCC Production Methods

Due to the high energy consumption, expensive raw materials, multiple production stages and release of CO_2 gases associated with PCC production using conventional methods, other production methods have been considered. The indirect carbonisation processes as reported by, Kakizawa et al. [19], is one method that have been considered. Here, the extraction of calcium is carried out on Wollastonite as it is rich in calcium, using acetic acid. This was considered as reports show that 0.21 kg CO_2/kg of PCC using the conventional method whereas, using this indirect acetic route, Wollastonite entraps about 0.34 kg CO_2/kg of PCC produced [20].

Another technique was developed by Kodama et al. [21] which is the pH swing CO_2 mineralization process where a recyclable reaction solution is used. This procedure consists of two steps where the first step is to extract calcium from a reaction of steel making slag and ammonium solvent by lower the ph. While in the second step, the pH is increased to enhance $CaCO_3$ precipitation.

One method that has been developed to pilot scale is the so-called slag to PCC process illustrated in figure 3.

Tested Solvents

Acids

- Acetic acid (CH_3COOH)
- Propionic acid (CH_3CH_2COOH)
- Nitric acid (HNO_3)
- Sulfuric acid (H_2SO_4)

Salts

- Sodium chloride (NaCl)
- Sodium acetate (CH_3COONa)
- Ammonium chloride (NH_4Cl)
- Ammonium acetate (NH_4COOCH_3)
- Ammonium nitrate (NH_4NO_3)
- Ammonium sulphate ($(NH_4)_2SO_4$)
- Ammonium di-hydrogen phosphate ($NH_4H_2PO_4$)
- Diammonium hydrogen phosphate ($(NH_4)_2HPO_4$)
- Aluminum sulfate ($Al_2(SO_4)_3$)
- Aluminum nitrate ($Al(NO_3)_3$)

Others

- Sodium hydroxide (NaOH)
- Urea $(NH_2)_2CO$)

(a)

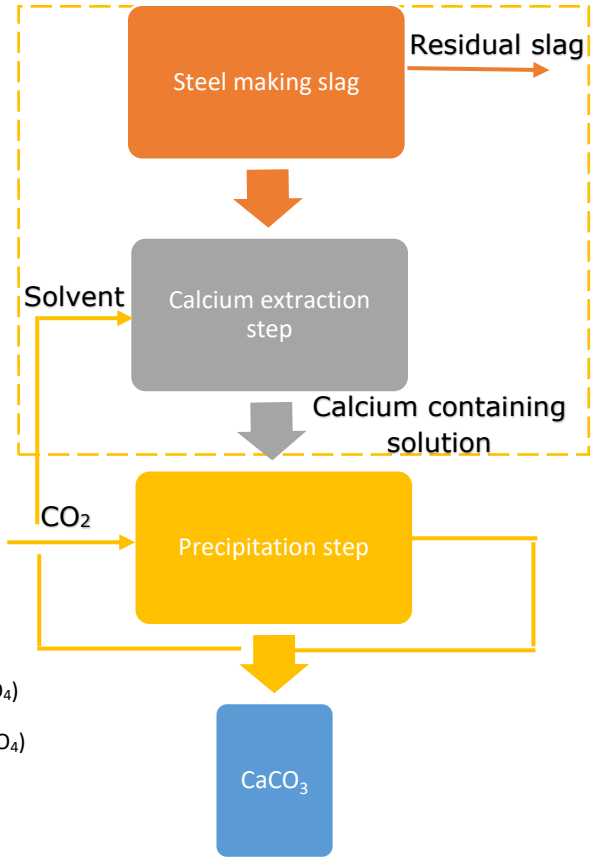

(b)

Figure 3. (a) Solvents tested as aqueous solutions for selective leaching of calcium from steel converter (basic oxygen furnace (BOF)) slags with three successful solvents highlighted. (b) Carbonation to produce PCC with the recycling of the leaching solvent [15].

As reported by R. Zenehoven [15], during the calcium extraction step, different solvents were tested to determine which is a more suitable solvent to get the most calcium extraction from the steel making slag. The three highlighted solvents (ammonium chloride, ammonium acetate and ammonium nitrate) were found to be more suitable solvents.

The PCC produced are tested for industrial quality, these proposed methods were studied to help utilize industrial wastes as well as reduce CO_2 emissions, but they also have some limitations as they mostly require additives, and the recycling of extraction agent have not been perfected.

1.3 Application of PCC

PCC is widely used in key industries, such as paper, plastics, pharmaceuticals, paints, and coatings etc. as seen in table 4 [22] . Starting from the mid-1980s, the high demand for PCC has always been due to the increased usage of PCC in the paper industry. Meanwhile, the production of paper is expected to continue increasing in the future, which will require increased growth demand for coating and filler materials. In Europe, Sweden and Finland are known to be huge manufacturers of paper and they continue to consume significant amounts of PCC. One of the biggest printing and writing paper producer- M-real's facility in Husum, Sweden (capacity 620 ktpy) has a satellite PCC plant operated by Imerys, since 2005 [23] .

Table 4 Applications of PCC in Europe [22].

Industry	%	Applications
Paper and Pulp	87	It is used as a filler and coating material to improve the paper's physical properties (brightness etc.).
Paints and Coatings	5	It is used to manufacture some emulsion paint and powder coatings as an anti-setting agent, and anti-rust agent. It is also used to give the paint a shiny look.
Adhesives and Sealants	5	Nano-sized PCC is a primary rheological additive in some high-performance sealants and adhesives to strengthen and reducing sagging.
Plastics	2	It is used as a filler, also to improve the strength, stiffness and stability, usually for rigid PVC and unsaturated polyesters. In plastic applications, the PCC surface is usually coated with surface agents to improve its hydrophobicity and dispensability in polymer matrices.
Cosmetics	<1	In the cosmetics industry, it is used to manufacture powders due to its free-

		flowing properties and fluffiness. It is also found in some toothpastes, creams etc.
Pharmaceuticals	<1	PCC is an active ingredient in calcium-based antacids. It can also be found in antibiotics which aids fermentation processes for pH control and flocculation.
Food Industry	<1	It is used as an additive, calcium support and fermentation aid.

With the recent data gathered, from 2020 to 2025, the PCC industry is expected to have a Compound Annual Growth Rate (CAGR) of 7% because of its unique properties which includes whiteness, brightness and opacity and its continuous increase in demand [24].

The highest demand of PCC seen in the paper and pulp industry. This is due to the growing demand for brighter and bulkier papers from the paper industries. PCC is also appreciated in this industry because it is an inexpensive filler material which when used at the wet-end of the paper-making machine, produces bright and smooth papers [24].

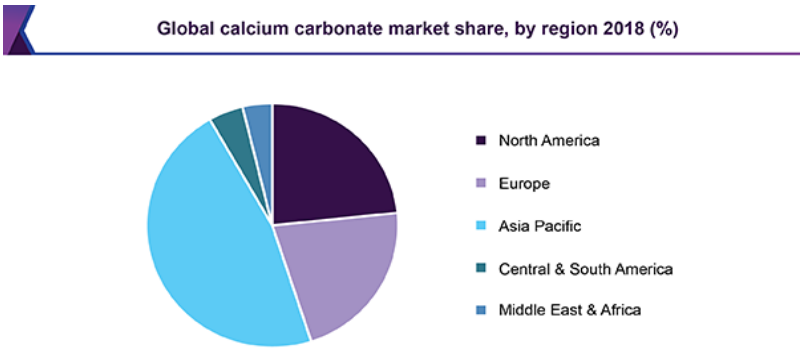

Figure 4 Global calcium carbonate consumption by region [25].

From market demand research, Asia-Pacific is leading the market in demand for PCC in the paper industry, where China is the leading consumer in this region [24]. In figure 4, the chart illustrates the consumption of PCC by region in 2018.

1.4 Quality Requirements for PCC

It is known that due to the different applications of PCC, the quality requirements will also differ, therefore, the intended market for the PCC is used to determine the quality requirements during the production process [26].

Some important qualities listed below:

i. Purity
ii. Morphology
iii. Specific surface area
iv. Particle size distribution
v. Brightness

Usually, PCC for commercial use should have a very high purity, generally above 97% - 99%. In addition, the brightness usually ranges from 94% - 99% [7].

The two main challenges faced in the quality requirements of commercial PCC are morphology and particle size distribution.

1.4.1 Morphology

Precipitated calcium carbonate has been reported by several authors to exist in three basic phases as shown in table 5: calcite (triagonal-rhombohedral), aragonite (orthorhombic), and vaterite (hexagonal) [27].

Calcium carbonate is known to have three anhydrous crystalline polymorphs (calcite, aragonite and vaterite) (table 2) and it can also be found in several hydrated forms (monohydrocalcite ($CaCO_3 \cdot H_2O$) and ikaite ($CaCO_3 \cdot 6H_2O$) also known as hexahydrate) [28][29][30]. The most common morphology for PCC is the hexagonal form known as calcite. Due to its thermodynamic stability under standard conditions and its ability to appear in different other morphologies (rhombohedral, scalenohedral, spheroidal, etc.), calcite has proven to be the most important polymorph in industrial applications. The next is aragonite, it is not so common, and it has a discrete or clustered needle orthorhombic crystal structure. The rarest and very unstable form of calcium carbonate is the spherical vaterite [31].

Table 5 Common availability of PCC polymorphs [27].

Polymorphs	Biological	Non-biological
Calcite	Very common	Very common
Aragonite	Very common	Rare
Vaterite	Rare	Rare

Calcite and Aragonite are mostly used for commercial purposes due to some of their attributes. Calcite is thermodynamically more stable over a broad range of temperature among the three polymorphs [27][32]. Calcite is mostly preferred in industries due to its superior appearance and the sparkly colour it gives the product when used as filler compared to others [33]. Aragonite is metastable at certain controlled temperature. The average refraction index of aragonite PCC is slightly greater than calcite. This attribute makes it a better filler material in comparison to calcite [34][35]. Vaterite rarely used due to its unstable state.

In recent years, nano-sized PCC (NPCC) has also been of interest in industries. It is often reported to be of spherical shape but also stated that other shapes exist. Nano PCC is usually used as a filler in polymeric materials with cost reduction being the optimal goal; it can also have beneficial impacts such as a higher impact resistance [36].

1.4.2 Particle size

For a high-quality PCC, the particle sizes are required to be very small (d_{50} ≤ 3 μm), but there are usually variations in the individual particle sizes from the laboratory processes. To account for these variations, the mean particle size is always given, as well as the particle size distribution (PSD). The PSD is very important in knowing the size and uniformity of the particles produced. Typical scales of mean particle size are usually d_{50}, which means 50% of the particles are this size and smaller, or d_{90}, which means 90% of the particles lie at this size or below.

In most industries, a very small particle size and narrow PSD are required. When PCC is used as a pigment in the paper industry, particle sizes of between 0.3 and 2.0 μm usually required with a very narrow PSD [12].

1.5 Previous studies and current approach

In recent research works, oil shale ash is being studied as a calcium rich material in place of limestone to produce PCC. By using this oil shale ash, some economic and environmental benefits can be achieved, for instance (CO_2 capture and storage, also, reduction of landfill wastes). In previous years, Velts et al. [37][38][39] carried out various experiments and published several papers on PCC production using the Estonian oil shale ash as the calcium rich material in ash - water systems. Stated below are some of the experiments and findings:

i. The first approach was in using oil shale ash for PCC production in the Ca^{2+} ion leaching process in a water suspension. Velts et al. [37] developed a model to characterize how the leachability changes and the equilibrium in the ash-water system between Ca^{2+} and other major ions as well as heavy metals. It was observed that there was a low leachability of heavy metals from the oil shale ash.

ii. Velts et al. [38] experimentally studied the mechanism of ash leachates carbonation in a stirred semi-batch barboter-type reactor by varying the CO_2 partial pressure, gas flow rate, and agitation speed. The derived result was used to develop several model equations to explain the precipitation process of $CaCO_3$ from OSA leachates. The qualities of the PCC produced from the experiment were also stated. High brightness PCC of ~96% with particle sizes ranging from 4 – 10 μm and controllable morphology (such as rhombohedral calcite or coexisting calcite and spherical vaterite phases) were obtained from the experiment under the mentioned conditions. In the production of PCC, the size, morphology, and purity of the PCC are very important in various applications. From the calculations they carried out, it showed that 1 tonne of ash (containing ~20% of free lime) can be used to produce up to 360 kg of $CaCO_3$, while during the carbonation process of $1m^3$ of leachates, at least 1.3 kg of CO_2 can be captured and up to 3.0 kg of PCC can be formed.

iii. Velts et al. [39] carried out another research using a continuous flow disintegrator-reactor to analyse the potential of producing PCC with different characteristics by using ash leachates, saturated with Ca^{2+} and accompanying ions (mainly SO_4^{2-} ions). As a result, PCC with a content of up to 99% $CaCO_3$ and mean particle diameter ranging from 3.7 – 7.5 μm at room temperature and atmospheric pressure was achieved. When the formed PCC was viewed using the X-ray diffraction analysis, it showed that the PCC was calcite with a minor infiltration of carbonate ions by SO_4^{2-} ions. With the scanning electron microscopy analysis, it was seen that the products can be produced with different shapes

and properties under different operating conditions. This confirmed it possible to produce crystals with the desired characteristics by controlling the operating conditions. In summary, ash leachate is a good material that can be used to produce PCC with specific properties demanded by target industries. The main obstacles that remained were – low Ca extraction efficiency in ash – water systems (due to low $Ca(OH)_2$ solubility in water) and PCC quality in terms of sulphur impurities and relatively big particle size.

The current approach focuses on using ammonium salt solutions (such as NH_4COOCH_3) instead of water in order to achieve higher Ca extraction efficiency and selectivity from oil shale ashes as well as higher quality of PCC in terms of morphology, brightness, size etc. compared to the previous approaches.

1.6 Crystallization

In this stage, several parameters have effects on the kind of PCC produced at the end of the experimental process. The crystallization process is usually carried out varying the temperature, pressure, amount of CO_2 and agitation speed. Crystallization occurs following three stages, which are:

i. Supersaturation: In this stage, the ions begin to cluster as ion concentration increases.

ii. Nucleation: Here, the ions grow as the concentration increases after which the ions will begin to arrange themselves into a regular shape. The rate at which nucleation occurs determines the PSD at the end of the experiment and so this should be taken into account and controlled [40].

iii. Growth: In this final stage, crystals are then formed from the nuclei. After the formation of the crystals, it continues to grow indefinitely until the experiment is ended [41].

With all these parameters, the crystallization occurs at different times and at different pH values, The PCC quality is then analysed for specific industrial usage.

1.7 Chemistry and reaction mechanisms

The reaction of Ca^{2+} extraction from lime and C2S is expressed as the main reactive components of oil shale ashes:

$$CaO_{(s)} + 2NH_4X_{(aq)} + H_2O_{(l)} \rightarrow CaX_{2(l)} + 2NH_4OH_{(aq)}\,\Delta H = -(83-88)KJ/mol \quad (1.6)$$

$$2CaO*SsiO_{2(s)} + 2NH_4X_{(aq)} + H_2O_{(l)} \rightarrow CaX_{2(aq)} + CaO*SiO_{2(s)} + 2NH_4OH_{(aq)}\,\Delta H = -(47-52)KJ/mol \quad (1.7)$$

Carbonization of Ca^{2+} solution and precipitation of $CaCO_3$:

$$2NH_4OH_{(aq)} + CO_{2(g)} \rightarrow (NH_4)_2CO_{3(aq)} + H_2O_{(l)} \quad (1.8)$$

$$(NH_4)_2CO_{3(aq)} + CaX_{(aq)} \rightarrow CaCO_{3(s)} + 2NH_4X_{(aq)} \quad (1.9)$$

The reaction mechanisms through which $CaCO_3$ is formed during the carbonation stage of a calcium rich solution that also contains an alkaline solution is described using the reactions below [42][43]:

i. Absorption of CO_2 gas into the solution

$$CO_{2(g)} \leftrightarrow CO_{2(aq)} \quad (0.10)$$

ii. Reaction of aqueous CO_2 with hydroxide ions to form bicarbonate.

$$CO_{2(aq)} + OH^-_{(aq)} \leftrightarrow HCO^-_{3(aq)} \quad (0.11)$$

iii. Continuous reaction of bicarbonate with more hydroxide ions to form carbonate.

$$HCO^-_{3(aq)} + OH^-_{(aq)} \leftrightarrow H_2O_{(l)} + CO^{2-}_{3(aq)} \quad (0.12)$$

iv. Reaction between the dissolved calcium and carbonate to produce $CaCO_3$.

$$CO^{2-}_{3(aq)} + Ca^{2+}_{(aq)} \leftrightarrow CaCO_{3(s)} \quad (0.13)$$

The reaction mechanism in step 1 occurs at the gas-liquid interface while the reaction mechanism in steps 2 - 4 occur in the bulk solution.

After this reaction mechanisms, other factors have been seen to affect the precipitation of $CaCO_3$ and they are discussed in the following sections.

1.8 Factors affecting $CaCO_3$ precipitation

In the precipitation of $CaCO_3$, and from several literature studied, some varying factors have different effects on the precipitation process which later determines the quality of the PCC produced. It is important to understand that some of these factors may be favourable or disadvantageous also in the extraction stage as it applies to the precipitation stage. The different factors affecting this precipitation have been outlined and will be briefly explained in the following sub sections.

1.8.1 System pH

Lots of research have been carried out to understand the effect of pH on the precipitation process. In an experiment carried out by Cheng et al. [44], it was seen that at a high pH level (> 12), the PCC morphology could no longer be controlled which resulted in irregular shapes. This was due to the high supersaturation level of the solution and it caused a decrease in the particle size as the nucleation rate of primary particles increased. According to the report of Hostomsky et. al. [45], it stated that the morphology of the PCC could affected by the pH of the solution during the precipitation process. They observed that the formation of vaterite PCC from calcium nitrate and sodium carbonate occurred at a pH > 9.5 but calcite occurred at a pH < 8.5.
Some other researchers stated in their works that a higher pH enhances the formation of aragonite. Kitamura et. al. [46] in their work produced aragonite PCC form a highly alkaline solution with a pH of 13.5.

1.8.2 Temperature

The effect of temperature on the production of PCC has be a critical part of the several research works carried out on the production of PCC. Temperature affects the morphology, the carbonation efficiency and even the time it takes the crystals to form. Some researchers observed during their experimental process that the higher the temperature, gas absorption becomes ineffective, and the CO_2 solubility becomes low. In this process, instead of the CO_2 to react to aid precipitation, a great amount of it escapes the solution in a gaseous form [47].

Kodama et al. In their own research also found that the higher the temperature, the less the absorption of CO_2, and at lower temperatures, CO_2 absorption increased. Hence, they proposed a maximum reaction temperature of 80˚C but noted that in the extraction stage, higher temperatures are favourable [21]. In their research, they also observed that temperature plays a major role in the morphology of the PCC produced. When the temperature was under 40 - 60˚C, cubic calcite was produced but as the temperature increased to about 90˚C, needle-like arogonite began to form [21].
Another researcher called Hubbe [48] also reported in his work that temperature has a great effect on the morphology of the PCC produced. He stated that, at lower temperatures, rhombohedral crystals are produced while at higher temperatures, scalenohedral crystals are formed. Opposing to his findings, Sun et al. [49] Stated in their own findings that at a higher temperature of 80˚C, rhombohedral crystals are produced while at a lower temperature of 20˚C, scalenohedral crystals are formed.

1.8.3 Agitation

As stated by Jones et al. [50], it was observed during an experiment that the agitation speed has noticeable effect on the crystals formed. In addition, Reddy et al. [51] observed in their study of calcite precipitation from supersatured solutions that the crystal growth rate constant was not determined by the stirring speed of the solution. Another important aspect to note on this is agitation can influence the particle size of the crystals through agglomeration process. It was observed that while moderate agitation can increase the rate at which agglomeration occurs by enhancing the collision frequency between particles, further increase in the agitation speed can cause shear and particle breakage thereby reducing the particle size [45].

1.8.4 Reactant concentration

From the research carried out by Jung et. al. [52], using $Ca(OH)_2$ and CO_2, it was observed that the crystal growth and particle size of the $CaCO_3$ can be affected by the presence of excess ionic content in the solution where the agitation is just right and mass transport is not a hindrance. They observed that when the stoichiometric conditions and concentration of ions were at the barest minimum during the carbonation process, the mean particle size of the crystals turned out in the desired size. The carbonation was observed under two conditions which were increasing the amount of CO_2 and reducing the Ca^{2+} ions and reducing the amount of CO_2 and increasing the Ca^{2+} ions, the particle size was observed to be small, and they concluded that the crystal

growth was inhibited by absorbing excess charged ions present in the reactants and hence, blocking growth regions on the surface of the crystals.
From several other research works [53][54], it was stated that, the higher the calcium concentration and the higher the pH, the formation of scalenohedral calcite is formed, but if Ca^{2+} ions concentration is low, then rhombohedral calcite is formed.

1.8.5 Electrical conductivity

One of the advantages of measuring the conductivity of the solution is; it gives a knowledge of the ionic content of that solution. It gives vital information about the total number of free ions (Ca^{2+}, CO_3^{2-}, Cl^-, NH_4^+ ions etc) present in the solution [55].

In addition, this electrical conductivity serves as an indicator to when the experiment should be stopped. Low conductivity indicates that Ca^{2+} ions have been bound, hence, there is a large amount of PCC recovered [55].

1.8.6 Residence time

Residence time plays a major role in the formation of PCC and their morphology. From various studied literature, it was seen that a shorter residence time in the carbonation process produces aragonite PCC. This is due to its metastable state, but if the aging time is increased, it transforms into calcite which also increases the particle size of the PCC formed due to Ostwald ripening [56]. On the contrary, as reported by Li et al. [57] longer the residence time (above 2 hours) favours the formation of aragonite while the shorter residence time favours the formation of calcite or vaterite. They carried out this experiment at room temperature and then concluded that the type of crystals formed may be due to the presence of NH^+ ions as impurities or just the length of the residence time.

1.8.7 Gas flow rate

As studied in several research works, the gas flow rate has been indicated as an important factor that influences the precipitation rate and has a role to play in the particle size of the PCC formed [58]. Agnihotri et al. [59] in their study stated that the particle size of the PCC decreases as the gas flow rate increases. This was due to the shear stress effect the flow rate had on the particles formed. Another research was done

by Feng et. al. [58] where the CO_2 bubble size (pore size varied between 17 – 40 or 101 – 160 μm) and the CO_2 concentration (25 and 100 vol%) were noted and it was observed in their experiment that the sizes of the particles were small with these parameters.
From other researchers also [60], the PCC size found to decrease as the gas flow rate increases, which is because of the increase in nucleation rate that facilitates breaking of the particles.

1.8.8 Bubble size

It was observed while carrying out the experiment that the particle size produced at the end of the experiment while using a filter that generated a smaller bubble size (less than 5.0 μm) as the CO_2 was bubbled in was not of the desired quality. Most of the PCC got entrapped in the mesh of the filter and it was observed that the smaller the bubble size, the smaller the particle size (usually 2 μm). In addition, this caused a significant delay in the time at which the precipitation occurred. When a filter with a larger mesh was used which allowed for bigger bubble sizes, the quality of the PCC produced was improved and the particle size was about 8 μm [61]. Also the precipitation occurred quickly compared to when the bubble sizes were small [62].

1.8.9 Seeding

From one of the reviewed literature, in the supersaturation process, it noted that the crystal growth rate is linearly dependent on the weight of seed crystal used to initiate growth [51]. In a process where the solvent solution is continuously recycled in a batch system or continuous process, there is a possibility that small particles left in the solution from the previous carbonation will be present as seed crystals and nucleation sites for the following carbonation processes if they are not first completely dissolved. This situation known as seeding.

1.8.10 Additives

Over the years, different kinds of additives have been used to monitor and enhance the crystal form (polymorphism) and the crystal shape (morphology) of PCC produced which has been difficult to achieve in an additive free system. In different surveys carried out, the additives that have affected the precipitation of PCC in their own ways are summarized below as reported by Jimoh et. al. [63].

Table 6 Summary of effect of different additives/surfactant on precipitated calcium carbonate syntheses [63].

No	Additives	Parameters	Effects	Synthesis process
1.	Poly acrylic acid (PAA)	20 - 45^{0}C pH – 4.5	Crystallization of irregular PCC particles	Carbonation [64] [65] [66]
2.	Ethylenediaminetetraacetic acid (EDTA)	25^{0}C 0.25 - 1% conc.	Formation of nanoparticle (PCC) 50 – 70 nm. Reduction of reaction time from 80 – 40 min	Carbonation [67]
3.	Zinc chloride (ZnCl)	25^{0}C 1% conc.	Formation of spherical nanoparticle size PCC (0,2 µm)	Carbonation [67]
4.	Magnesium chloride ($MgCl_2$)	25^{0}C, 1% conc. 25^{0}C, 75% conc.	Spindle and spherical-shaped PCC Single phase aragonite PCC	Carbonation [68]
5.	Citrate and malate		Rod-like shape aragonite PCC	Solution [68]
6.	Phthalic acid		Rhombohedral shape aragonite PCC	Solution [68]
7.	Sodium dodecyl sulfate (SDS)		Calcite with vaterite PCC	Solution [69]
8.	Dodecyltrimethylammonium bromide (DDTAB)		Increase transformation from vaterite to calcite with a reduction in crystal growth rate	Solution [69]

9.	Poly (*N*-vinyl-2-pyrrolidone) PVP	High conc.	This favours the formation of calcite PCC and inhibits the formation of vaterite	Solution [70]
10.	Ammonium citrate	0.3 m/L, 10^0C	Calcite PCC produced (40 – 90 nm)	Solution [71]
11.	Polydiallyldmethylammonium chloride (PDDA)	1 g/L, 30 - 50^0C 90^0C 0.1 g/L, 90^0C	Rhombohedral calcite PCC Rectangular prism calcite PCC (10 µm) 25% aragonite PCC	Solution [56]
12.	Cetyl trimethylammonium bromide (CTAB)	1 g/L, 30 - 50^0C 0.1 g/L, 90^0C	Calcite PCC 19% aragonite	Solution [56]
13.	Ethylenediaminetetraacetic acid (EDTA)	0.1 g/L, 30 - 70^0C 0.1 g/L, 90^0C 2.0 g/L	100% calcite 27% aragonite PCC 100% calcite PCC	Solution [56]
14.	Carboxylmethyl chitosan (CMCS)	1000 ppm 10000 ppm	Spherical PCC particles Peanut PCC shape	Solution [72]
15.	Dodecyl sulfonate (DDS)		Calcite PCC	Solution [73]
16.	Sodium dodecyl benzenesulfonate (SDBS)		Vaterite PCC	Solution [73]
17.	Non-ionic dextran	30 - 45^0C	Rhombohedral and scalenohedral calcite PCC	Carbonation [74]

18.	Poly (*N*-vinyl-2-pyrrolidone) PVP	0.0005% conc. 0.005% 0.05%	Calcite PCC Aragonite PCC Calcite + aragonite PCC	Solution [75]
19.	Glycerol	20%	Calcite PCC with particle size of 0.1 – 0.59 μm	Carbonation [76]
20.	Isopropyl alcohol and *n*-butanol		Calcite PCC with a size of 2.5 μm	Carbonation [76]
21.	Polyacrylamide	0.50 - 50%	Calcite PCC produced	Solution [75]

1.9 Aim of the study

The aim of this work is to study the effect of operating parameters and additives on PCC precipitation efficiency and quality in oil shale ash (OSA) based PCC production. The literature review was carried out to select the parameters (temperature, pressure, gas flow rate, additive etc) favourable for the experimental procedure. The experimental part was carried out for understanding how the selected process parameters affect or enhance the quality (morphology and particle size) of the PCC produced. The Aspen plus modelling was implemented to assess the process material and energy consumption and oil shale ash based (OSA) PCC production potential through thermodynamic calculations and process modelling.

As a result, the key process parameters were chosen and their effect on PCC precipitation efficiency and PCC quality estimated.

2. Experimental part

2.1 Materials and methods for sample preparation

The experiments were carried out in various stages at a laboratory scale. Table 7 below represents the main steps and analysis procedure of the experiment.

Table 7 Outline of the investigated procedures

No.	INVESTIGATED PROCEDURES
1.	Leaching and dissolution behaviour of the ash-NH_4COOCH_3 system. Ca^{2+} ions extraction from ash-NH_4COOCH_3 in a batch process.
2.	Addition of $NaHCO_3$ to enhance the precipitation process.
3.	Carbonation (Precipitation process) in the gas-liquid system. CO_2 absorption by Ca^{2+} ions rich leachates.

2.2 Precipitation of $CaCO_3$ in CO_2-oil shale ash-NH_4COOCH_3 system with additives

This experiment was done at a laboratory scale using a batch reactor. In this process, 100 ml of calcium rich solution gotten from the OSA mixed with NH_4COOCH_3 solution and $NaHCO_3$ was put in a reactor and CO_2 gas was bubbled into it, the precipitation of the $CaCO_3$ was carried out at room temperature, same agitation speed and different amounts of CO_2 introduced into the reactor. This was done to compare the different qualities of PCC produced under each condition.
Figure 5 illustrates the leaching and the carbonation process to produce PCC.

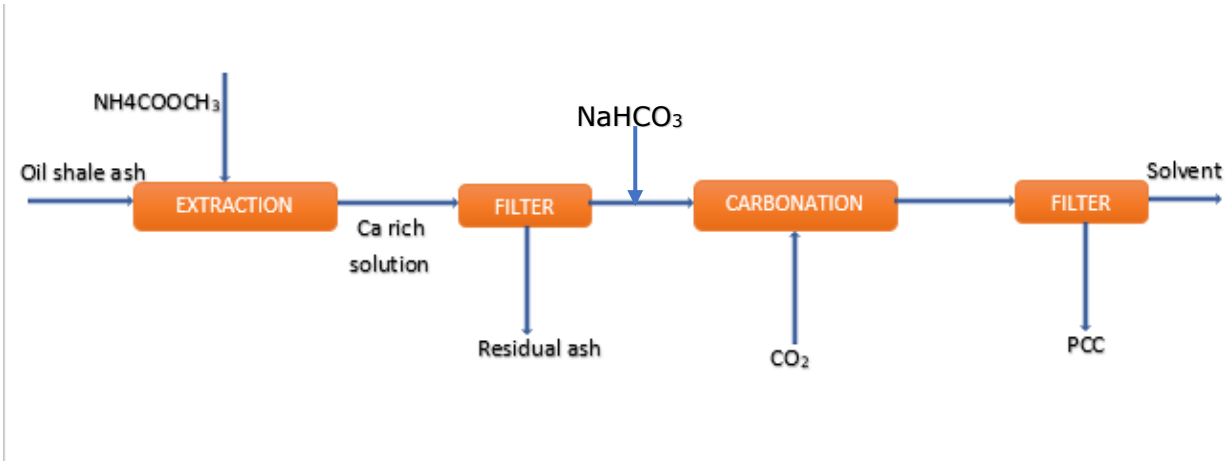

Figure 5 Precipitation of $CaCO_3$ in CO_2 - oil shale ash - NH_4COOCH_3 system with additive

2.3 Characterization of oil shale ash

The oil shale ash (OSA) used for this experiment was gotten from the Auvere power plant, Estonia. The ash gotten was the Auvere mix from fly ash and general ash. The characterization of this material gives a proper knowledge of the properties and composition of this material which will help in understanding the behaviour and results gotten from the experimental analysis.

XRD analysis was ordered from the University of Tartu, Department of Geology to get the phase composition and the result is present in Figure 6.

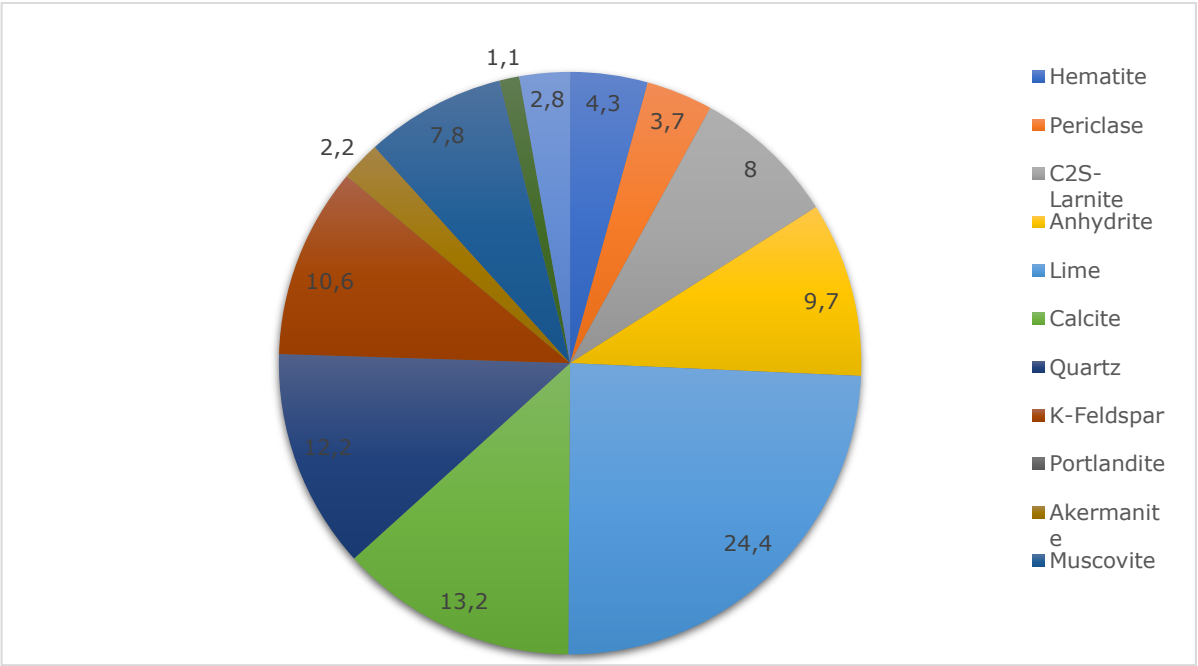

Figure 6 Phase composition of oil shale ash from Auvere PP, %

The chart represents the main components found in the investigated OSA during the XRD analysis. The lime (CaO), portlandite ($Ca(OH)_2$) and larnite (C2S) are the major components that are considered during the extraction of Ca^{2+} ions. The anhydrite ($CaSO_4$) and hematite (Fe_2O_3) values are usually hoped to be little due to the release of SO_4^{2-} ions from anhydrite and Fe^{3+} ions from hematite which could after the quality of the final product.

The chemical composition of the OSA was also determined using the Rigaku ZSX Primus II at the University of Tartu, Department of Geology. Figure 7 shows the elements as oxides present.

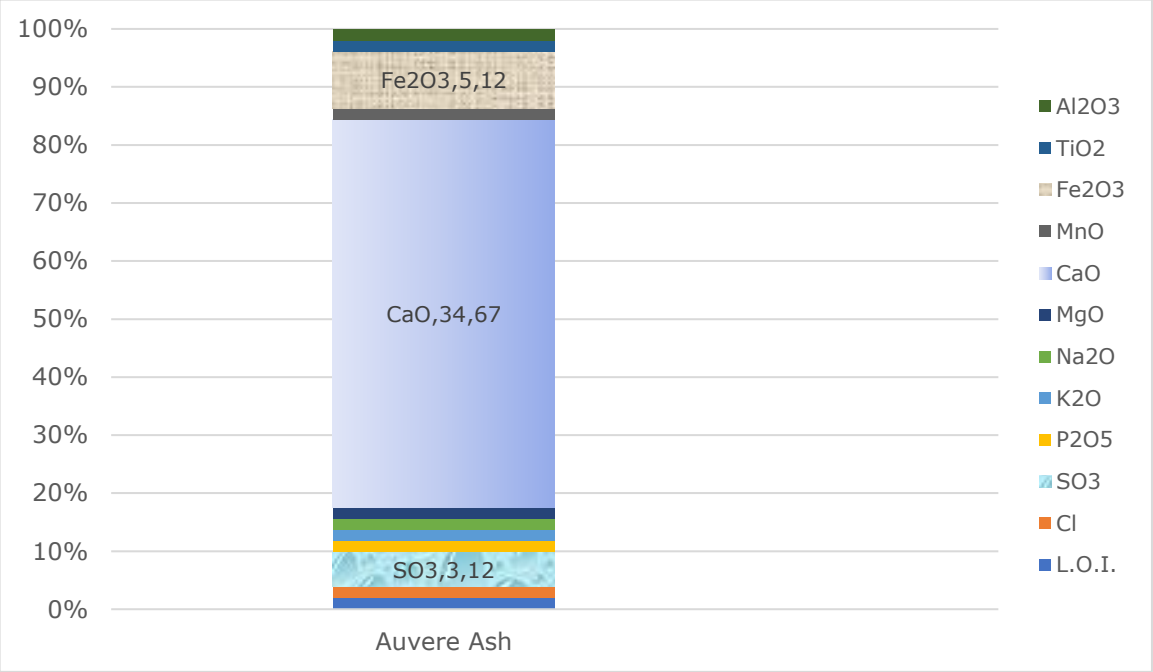

Figure 7 Chemical composition of oil shale ash

The CaO, Fe_2O_3, and sulfur as SO_3 are the major components in the OSA when analysed with the XRF device.

2.4 Analysis characterization

The characterization which includes composition, morphology, surface area and particle size of the solid products (oil shale ash and precipitated calcium carbonate, $CaCO_3$, as PCC) and liquid parameters were derived using the following methods outlined in tables 8-11 below.

Stage 1. Here, all the solid and liquid analyses to be carried out are first listed out with the equipment used.

Table 8 General analyses

Stage 1	Analyses (Solid and liquid phases)
Material Characterization	Equipment
XRD (Phase composition)	Brucker D8 Advanced (University of Tartu, Department of Geology)
XRF (Elemental composition)	Rigaku ZSX Primus II (University of Tartu, Department of Geology)
Total Carbon	ELTRA CS-580 Carbon/Sulfur Determinator.
Free CaO	ELTRA CS-580 Carbon/Sulfur Determinator
Size Distribution	HORIBA Laser Scattering Particle Size Distribution Analyzer LA- 950
Specific Surface Area	Sorptometer Kelvin 1042
System pH and EC	METTLER TOLEDO SevenGO Duo pro
Ca^{2+}, Mg^{2+}, Fe^{3+}	The Varian SpectrAA 55B atomic absorption spectrometer
SO_4^{2-}, SO_3^{2-}, SiO_2	Lovibond SpectroDirect
SEM (Morphology)	Zeiss EVO MA15 (University of Tartu, Department of Geology)
Purity	ICP-MS, Agilent 8800x (University of Tartu, Department of Geology)

Stage 2.

Calcium (Ca^{2+} ions) extraction analyses was done in this stage. The different analyses carried out in the solid and liquid phases with the equipment used are listed in table 9.

Table 9 Ca^{2+} ions extraction analyses

Ca^{2+} Extraction	Solid Phase	Equipment	Liquid phase	Equipment
	XRD	Brucker D8 Advanced (University of Tartu, Department of Geology).	System pH and EC	METTLER TOLEDO SevenGO Duo pro
	TC/TIC	ELTRA CS-580 Carbon/Sulfur Determinator.	Ca^{2+}, Mg^{2+}, Fe^{3+}	The Varian SpectrAA 55B atomic absorption spectrometer
			SO_4^{2-}, SO_3^{2-}, SiO_2	Lovibond SpectroDirect

Stage 3.

Carbonation material analyses was carried out in this stage and the solvent was analysed to understand its properties before it was used in the experiment.

Table 10 Carbonation material analyses

Carbonation (Liquid phase)	Equipment
System pH and EC	METTLER TOLEDO SevenGO Duo pro
Ca^{2+}, Mg^{2+}, Fe^{3+}	The Varian SpectrAA 55B atomic absorption spectrometer
SO_4^{2-}, SO_3^{2-}, SiO_2	Lovibond SpectroDirect

Stage 4.

In this final stage, the PCC derived from the experiment is analysed using the following equipment to determine the quality of PCC produced.

Table 11 Product (PCC) analyses

Analyses	Equipment
Morphology (SEM)	Zeiss EVO MA15 (University of Tartu, Department of Geology)
Particle Size Distribution	HORIBA Laser Scattering Particle Size Distribution Analyzer LA- 950

The equipment used during the solid and liquid phase analyses are briefly described in the sub-sections below.

2.4.1 X-ray fluorescence spectroscopy (XRF)

The XRF ((Rigaku Primus II) at the Department of Geology, University of Tartu was used to measure the chemical composition of the OSA sample used during the experiment. The relative chemical composition of the elements present in the ash are represented in Figure 7.

2.4.2 X-ray powder diffraction spectroscopy (XRD)

This equipment is used to carry out analytical analysis of the phase composition of the OSA used during the experiment. The Bruker D8 Advanced at the Department of Geology, University of Tartu was used for this. The values of the elements found present in the sample are represented in table 18.

2.4.3 Total carbon content (TC)

The analysis was done using the ELTRA CS-580 carbon/sulfur determinator. First the machine is heated to 1100^0C and oxygen gas is introduced into the machine at a pressure of 1.5 bar. It is calibrated (12% C and 43.7% CO_2) using ELTRA powder. The ash is measured and weighed (typically 2.0 – 2.5 g) and then pushed into the carbon/sulfur determinator for analysis where the carbonates decompose.

The result of the measurement is gotten in C% from which the mineral CO_2 content is calculated with the formula below.

$$CO_2 = \frac{(44 \times C\%)}{12} \quad (2.1)$$

If as calcium carbonate ($CaCO_3$)

$$CaCO_3 = \frac{CO_2 \times 100}{44} \quad (2.2)$$

2.4.4 Total inorganic carbon (TIC)

This analysis was also done using the ELTRA CS-580 carbon/sulfur determinator which was set to a temperature of 100^0C and a pressure of 1.5 bar. Ash weighing between (2.0 – 2.5 g) was measured into a glass bottle connected to an oven (250°C) and 6 ml of 50% phosphoric acid was pumped into the bottle and stirred at a speed of 400 rmp. The CO_2 and $CaCO_3$ values were calculated using the formula in (2.1 and 2.2).

2.4.5 Particle size distribution (PSD)

The particle size was measured using the HORIBA Laser Scattering Particle Size Distribution Analyzer LA-950. The diameter median, mean and mode size of the particles were measured. The diameter median can be described as the mid-point that serves as a boundary between the finer particles (d_{10}) and the coarse particles (d_{90}). This is denoted as d_{50}. The mode size is the grade of particles that makes up a larger percentage of the sample.

2.4.7 Norm of CO_2

This is the amount of CO_2 added to the reaction mix during the experiment. It can also be described as the ratio between the CO_2 does and the volume of solution in the reactor. This is dependent on the bubble size. The smaller the pore size of the barboter (16 – 40 μm), the smaller the amount of CO_2 doses. Using a barboter with a larger pore size (100 – 160 μm) also increases the amount of CO_2 added by approximately 2 times [61].

2.4.8 Free CaO content

To determine the value of the free lime (CaO) present in the ash, ethylene glycol was used. Approximately 0.5 g of ash was mixed with 50 ml of ethylene glycol in a 100 ml flask and put into a water thermostat at a temperature of 60^0C and left to heat for about 30 minutes. The suspension was also shaken at time intervals before the procedure was completed. After the 30 minutes, the suspension was filtered using a vacuum pump and filter paper (2 – 3 μm). The resulting solution was then titrated using 0.1 M of hydrochloric acid (HCl) and methyl red as an indicator, this was done until the red color appeared [78].

The formular for calculating free CaO content is shown below.

$$CaO = \frac{V_{HCl} \times 0.1N \times 28.04 \times 100}{1000 \times m_{ash}} \quad (2.4)$$

If expressed as calcium hydroxide ($Ca(OH)_2$)

$$Ca(OH)_2 = \frac{CaO \times 74}{56} \quad (2.5)$$

2.4.9 pH and electrical conductivity

These liquid analyses were done using the METTLER TOLEDO SevenGO Duo pro. The measurements were carried out on the parent ammonium solution, the leachate, and the carbonation solution. The pH electrode was first calibrated to (4.01, 7.00 and 9.23) respectively before it was used to measure the solutions. The electrical conductivity sensor was also calibrated to a standard of 12.88 mS/cm before it was used to measure that of the solutions.

2.4.10 Analysis of Ca^{2+}, Mg^{2+}, Fe^{3+} ions concentrations

Ca^{2+} ions present in the solution were determined using the Varian SpectraAA 55B atomic absorption spectrometer. The instrument was first calibrated correctly (Method A.W. 40,08) for accuracy purposes. Other parameters set were the wavelength (422.7 nm) and the lamp power (10 mA). The flame which was used to atomize the sample was derived from a mixture of combustible gas(acetylene) and oxidizer (air).

10% of strontium chloride was added to the diluted portion of the solution to eliminate compounds that inhibit calcium absorption ($CaSO_4$). When this was done, the first step was to determine the calibration curve after which the samples were analysed. Magnesium (Mg^{2+}) ions were seen at (method A.W. 55,85) and iron (Fe^{3+}) ions were seen at (method A.W. 24,31).

2.4.11 Analysis of SO_4^{2-}, SO_3^{2-}, Si concentrations

The sulphate ions (SO_4^{2-}) were determined using the Lovibond SpectroDirect device. Before the analysis, the solution was diluted to about 10timess the original state and the detection range of the device was set between 2 – 100 mg/L. 10 ml of the solution was put into a little bottle using a pipette, then it was put into the device and zeroed (Method 360). It was then brought out and Vario Sulfa 4F10 ml powder was added to the solution to help determine the sulphate ions present in the solution. The bottle was put back into the Lovibond device and the analysis lasted for about 5 minutes before the results were obtained.

The sulphite (SO_3^{2-}) ions (method 370) and silicon (method 350) contents in the solution were also determined using the same Lovibond device. The result of the silicon content can be calculated with the formula below.

$$Si = SiO_2 \times 0.47 \quad (2.6)$$

2.5 Measuring solution characteristics

Measurements of the dynamic viscosity, density, diffusion coefficient, specific heat capacity and the thermal conductivity of the calcium rich solution gotten from the mixture of OSA and NH_4COOCH_3 solution were investigated to have an in-depth knowledge of the characteristics of the solution used for carbonation, as well as to

determine certain parameters useful for modelling the process. As a reference, measurements were also made on a pure 2 M NH_4COOCH_3 solution at 25°C, to understand the characteristics of the solution used for the extraction process and for understanding the effect that calcium ions have on the solution.

The dynamic viscosity of the calcium rich solution was measured using a Hoppler viscometer with Julabo heating circulator, aerometers, and thermometers at 20, 25, 30, 35, 40 and 45°C. Additionally the dynamic viscosity of the reference NH_4COOCH_3 (2 M) solution was measured, also that of deionised water for calibrating the machine, and the calcium rich solutions (OSA extraction). The device was equipped with its own heating system for increasing the temperature of the fluid samples. Two measurements were made for each sample at each temperature and an average was taken.

Figure 8 Hoppler viscometer with Julabo heating circulator used for measuring liquid viscosity.

The density of the ball used inside the hoppler viscometer is (ρ = 2.222 g/cm^3) with a constant of (k = 0.009494).

Figure 9 Ball used for determining the viscosity of each liquid.

The values of each sample were determined using the formula below and results are seen in table 12, and the formula what was used is following:

$$\eta = k * (\rho_1 - \rho_2) * t \quad (2.7)$$

η - viscosity

k - ball constant

ρ1 – ball density

ρ2 – density

t – time

3. Results

3.1 Ca extraction in oil shale ash-NH_4COOCH_3 system

In the process of extracting the available calcium (mainly as lime and C2S) in the OSA, the extraction process is carried out in the LARA™ controlled lab reactor where the ash is mixed with NH_4COOCH_3 solution during 1 hour at ambient temperature, atmospheric pressure, and a stirring speed of 600 rpm, after which the calcium rich solution is separated from the ash residue by filtration. The next process is the carbonation stage, where CO_2 containing gas is introduced into the calcium rich solution, choosing operating parameters depending on the desired morphology to be achieved.

NH_4COOCH_3 is a preferred solvent as compared to using water mainly due to because it has some advantages over water. For example, using NH_4COOCH_3 as the solvent, little amount of sulphate (~0.2) was detected in the calcium rich solution after the mixture has been filtered unlike when water is used, there are large amounts of sulphate (~0.75) present in the calcium rich solution. The main advantage is that the NH_4COOCH_3 enhances the extraction of the calcium content from the OSA compared to using water as the solvent multiple times. Figure 10 below shows the calcium extraction process as overall.

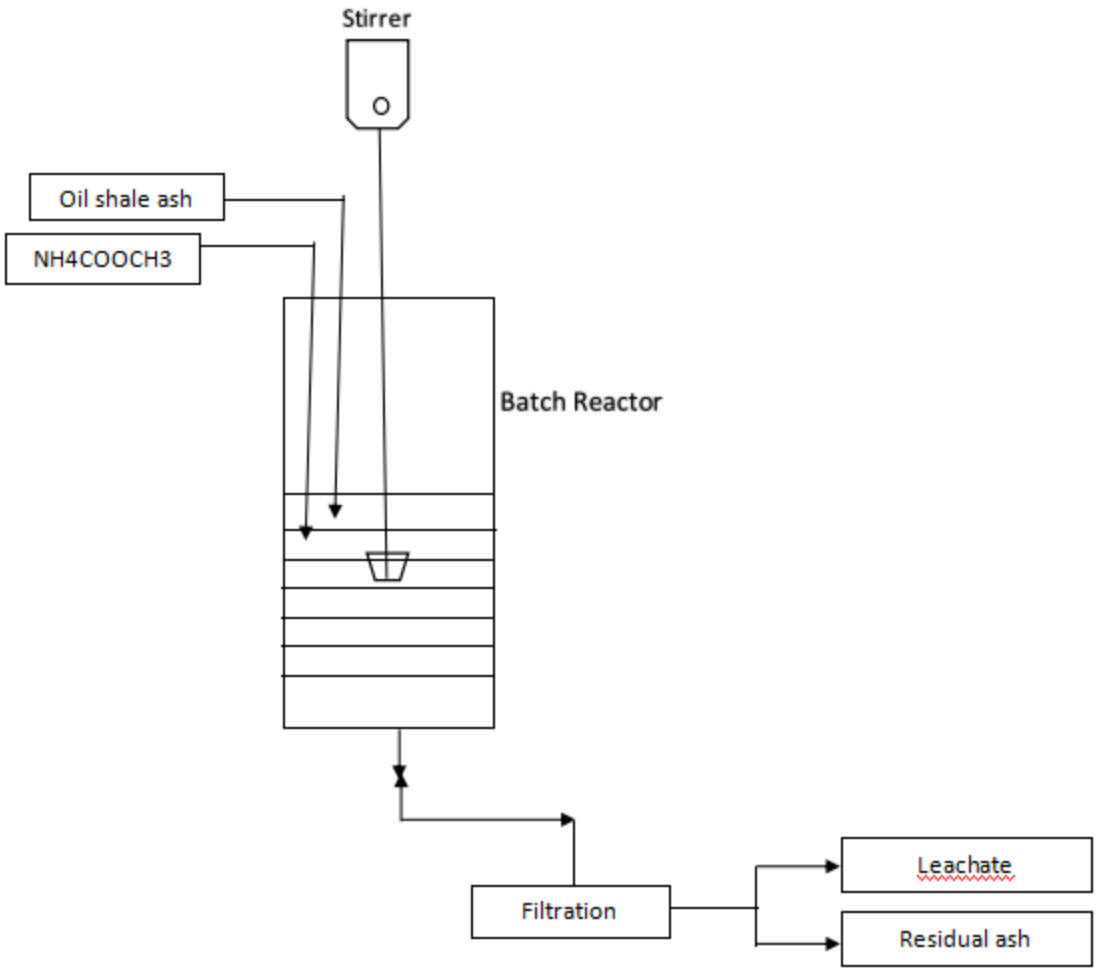

Figure 10 Leaching process to extract the calcium rich solution from the OSA and NH_4COOCH_3 solution.

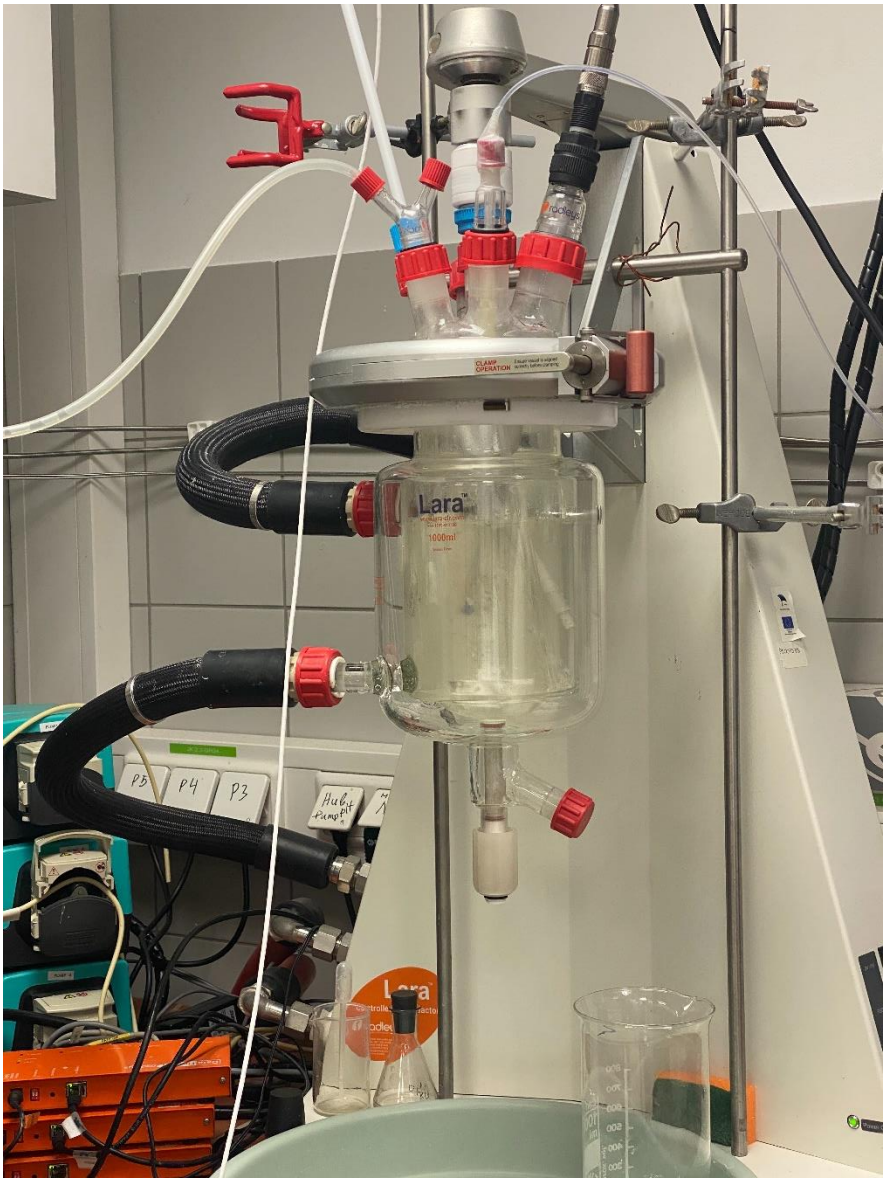

Figure 11 LARA™ controlled lab reactor used for leaching and carbonation experiments.

This ash was again tested different conditions to study the effect of operating temperature, mixing speed and liquid to solid ratio on Ca extraction efficiency. It was observed then from the results that the extraction efficiency is mainly affected by liquid to solid ratio and operating temperature. Increasing temperature from 20°C to 75°C enhanced the extraction efficiency of Ca^{2+} ions where Eca(total) increased from 32 to 50% while ECa(CaOf+C2S) increased from 53 to 81%.

Ca^{2+} extraction efficiency was calculated as follows:

$$E_{Ca}(total) = \frac{Ca^{2+} * V * 100\%}{mol_{CaO}\ (total) * M_{Ca^{2+}}} \quad (3.1)$$

Under active ash Calcium:

$$E_{Ca}(vCaO + C_2S) = \frac{Ca^{2+} * V * 100\%}{mol_{CaO}\ (vCaO + C_2S) * M_{Ca^{2+}}} \quad (3.2)$$

After the leaching procedure was completed, the viscosity of the solutions was also measured, the solutions measured were the calcium rich solution and NH_4COOCH_3 and the viscosity of water was used as a reference. The viscosities of these solutions are presented in table 12 and figure 12.

Table 12 Viscosity values (mPa*S*cm^3)

Temperature ℃	**Water**	**NH_4COOCH_3**	**Ca^{2+} rich extract**
20	0.9295	1.4862	2.0148
25	0.8839	1.3739	1.6258
30	0.7917	1.0236	1.5150
35	0.7578	0.9342	1.4252
40	0.7239	0.8780	1.0558
45	0.7017	0.8216	0.9892

The comparison between each sample can be seen in the graph in figure 12.

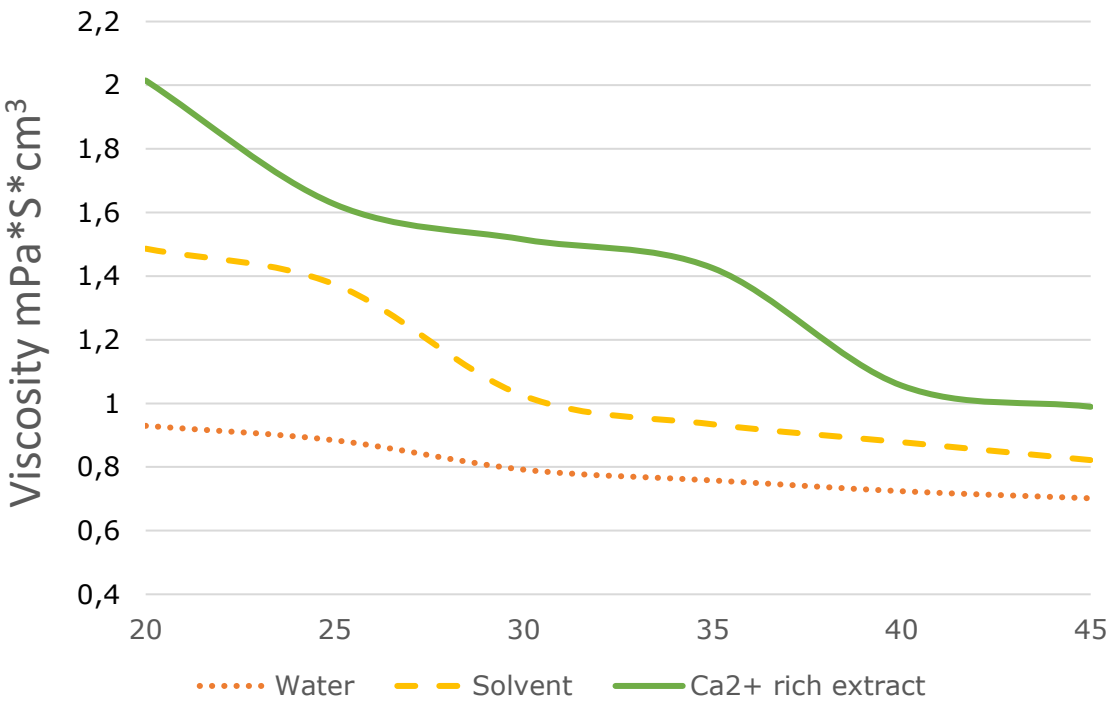

Figure 12 Comparison between the viscosities of Water, Solvent and Ca^{2+} ion rich extract.

The according data could be used in for further studies.

3.2 Carbonation procedure

Carbonation experiments were carried out in two experimental plan system for comparison: (i) Pure extract as Ca^{2+} rich solution and (ii) Ca^{2+} rich solution mixed with $NaHCO_3$. During the process of the experiments in system (i), 100 L/h of CO_2 containing model gas (15% CO_2 and 85% air) was bubbled into the solution in some parts of the carbonation process while in the remaining, 100% CO_2 gas was used. The experiment lasted above 60 minutes in case of using 15% CO2 gas while in the case of using 100% CO_2 gas, the experiment ended much quicker. The experiment in system (i) was ended when the pH value was between 7.1 – 7.5 but it later increased after filtration due to cooling. In system (ii), the experiment lasted up to 15 minutes, however the carbonation did not end in every test after the pH became stable. The time at which the PCC started forming was recorded. It was observed in the experiment that the PCC formed very quickly due to the addition of the $NaHCO_3$ salt in system (ii) as compared to the experiment carried out in system (i) without the addition of $NaHCO_3$.

After the carbonation experiment was done, the PCC was separated from the solution by filtration. The electrical conductivity and the pH of the resulting solutions were measured. Ca^{2+}, SO_4^{2-}, SO_3^{2-} ions values were also measured from the solutions.

The resulting PCC was dried (105°C, at least 3 h), and the weight was measured. Also, the total carbon (TC) content, the particle size distribution (PSD), purity, and the morphology were also determined-. The morphology was determined using SEM in the case of (i) system. In case of (ii) the produced PCC were washed several times to leach out the Na^+ ions. And the products were analysed before and after washing.

Table 13 Carbonisation procedure for system (i) without the addition of $NaHCO_3$

No	Initial solution	Temp	Rpm	CO_2 %	Initial pH	pH when crystals occurred	Final pH (filt)	Start time (crystal appearance)	End time	Ca^{2+} content g/L	EC mS/cm (filt)	Ecarb	PSD (um) (dmedian)
1.	Lara_extr	20	200	15	10.31	9.94	7.75	41.6	173.7	19.47	75.17	64.46	0.94
2.	Lara_extr	20	200	100	10.24	-	7.89	16.42	42.76	19.47	78.49	73.86	2.27
3.	Lara_extr	20	600	15	10.31	9.9	7.80	30.33	106.35	19.47	76.59	67.49	1.69
4.	Lara_extr	60	200	100	9.14	9.01	8.13	0.86	28.97	19.47	75.01	66.82	9.09
5.	Lara_extr	60	600	100	9.12	9	9.42	0.22	24.76	19.47	61.09	34.67	3.60

Data source: Lara Carb experiment

In the next stage of the experiment, $NaHCO_3$ was added to the Ca^{2+} rich solution before the CO_2 gas was bubbled into it (Table 14). The resulting data for PCC purity as well are seen in table 14.

Table 14 Carbonisation procedure results for system (ii) with the addition of $NaHCO_3$

No	Temp	RPM	Ca^{2+} content in extraction (g/L)	$C0_2$ %	Gas flow rate (L/h)	$NaHCO_3$ addition mol/L	Norm of CO_2	Time (min)	End pH	EC mS/cm	SO_4^{2-} g/L (filtrate)	PSD (µm) (Before washing)	PSD (µm) After washing	$CaCO_3$ %
1	Room	~800 rpm (stirrer nr 5)	11.35	15	100	0.2	2	5	8.416	97.9	0.2265	12.737	12.786	98
2			11.35		100	0.2	6	15	8.441	99.5	0.181	9.715	8.521	97
3			11.35		100	0.7	2	5	8.733	98.8	0.1489	7.160	7.708	98
4			11.35		100	0.7	6	15	8.646	97.6	0.2005	8.364	11.126	99
5			26.5		200	0.2	2	5	8.522	96.3	0.125	10.936	9.443	97
6			26.5		200	0.2	6	15	8.441	97.1	0.1595	13.048	11.805	95
7			26.5		200	0.7	2	5	9.000	94.9	0.193	9.805	10.866	95
8			26.5		200	0.7	6	15	8.767	96.2	0.2005	9.032	10.699	92
9			26.5		150	0.5	4	10	8.723	97.3	0.1755	5.498	-	97
10			26.5		150	0.5	4	10	8.699	96.7	0.1765	5.493	5.257	97

Data source: Carb experiment

The images of the dried PCC for system (ii) before washing and after washing are shown below in figure 13a and b.

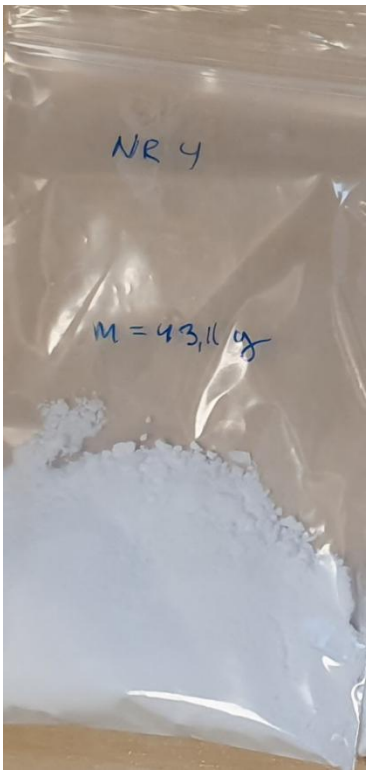

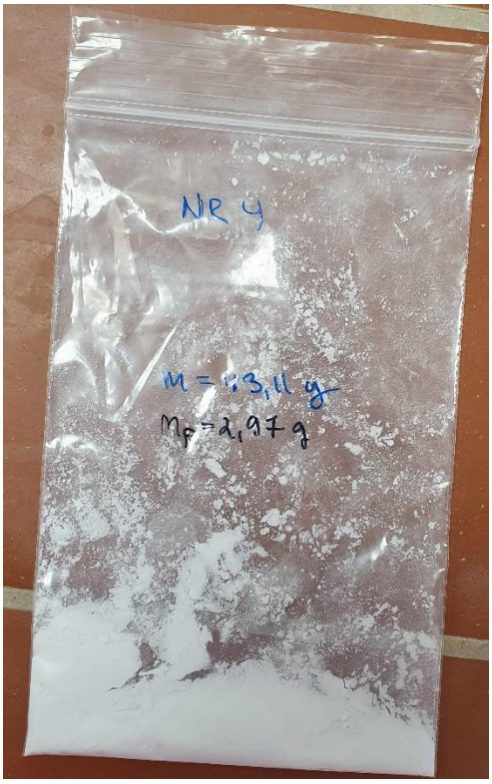

Figure 13 (a) Before washing (b) After washing.

After washing, the real PCC amount was gotten, and the product weight dropped from 43.11 g to 2.97 g. Latter means that instead of PCC, mainly precipitated the additive, which had to be washed out. The same applies to the other images.

3.3 Effect of selected parameters on carbonation efficiency

3.3.1 Reactant concentration

The concentration of the reactants (2 M NH_4COOCH_3, L/S = 5) had a major role to play in the carbonation efficiency as these values were concluded to be favourable in both systems. It was observed that when the concentration of the Ca^{2+} ions rich solution was reduced, the carbonation efficiency dropped and when it was increased, the carbonation efficiency also increased for system (i) as represented in table 13. Therefore, it was concluded that high concentration of the reactant (Ca^{2+} ions rich solution) gives a favourable result.

The carbonation efficiency was calculated as follows:

$$E_{carb} = (1 - [Ca^{2+}])/[Ca^{2+}]initial * 100\% \quad (3.3)$$

3.3.2 Additive concentration

During the experimental procedure in system (ii), when $NaHCO_3$ (0.2 – 0.7 mol/L) was added to the calcium rich solution and CO_2 gas was bubbled into the solution, it was observed that a precipitate occurred almost as soon as the experimental procedure started. This procedure lasted between 5 - 15 minutes as compared to previous studies where the procedure took about 1 hour before the PCC stared forming. It was observed that the higher the amount of the additive, the faster the precipitate appeared. Later we learned that it was mainly the additive that precipitated not PCC and it needed several washing cycles to get pure PCC.

The final Ca^{2+} ion concentration could not be measured directly from the solutions using (Method A.W. 40,08) after carbonation due to the over saturation of Na^+ ions in the solution. Hence, precipitation efficiency based on initial and final Ca^{2+} ions concentration could not be analysed.

3.4 Effect of selected parameters on product quality

The different selected parameters such as additive concentration, reactant concentration etc. had significant effects on the particle size and morphology of the PCC obtained after the experiment in system (ii) while in system (i), the solvent concentration, reactant concentration were the factors considered.

3.4.1 Particle size distribution (PSD)

The reactant concentration, solvent/ash ratio = 5, and solvent concentration (2 M NH_4COOCH_3) choice had great influence on the particle size distribution of the PCC produced in system (i) without the addition of $NaHCO_3$ while in system (ii), the addition of $NaHCO_3$ had its influence in the PSD of the product.

In system (i), increasing the mixing speed was observed to decrease the particle sizes of the PCC (at 20^0C, CO_2 15 - 100%). When the operating temperature was increased from 20 - 60^0C and reducing the CO_2 concentration (15% CO_2), the size of the PCC increased from 0.3 – 13 µm.

Increasing operating temperature from 20 - 60^0C and increasing the CO_2 concentration, (100% CO_2) the size also increased from 1 - 4 µm.

While under the optimal conditions (40^0C and 400 rpm), with 15% CO_2 concentration, the size was 4 µm and when 100% of CO_2 was used, it was 4 µm.

This showed that at higher temperatures and higher CO_2 concentration, larger particles were produced.

From the result of the experiment carried out in system (ii) with the addition of $NaHCO_3$, it was observed that the particle size (dmedian) of the PCC produced during the 10 runs ranged between 5 µm – 13 µm, they turned out bigger as reported in table 14 under constant operating conditions (room temperature and 15% CO_2). The results from the 10 runs are represented in figure 14.

Comparing the peaks of the particle sizes in systems (i) and (ii), it was observed that in system (i), the particle size of PCC was generally smaller but more influenced by agglomeration. In system (ii), with the addition of $NaHCO_3$, the particles were generally bigger, but the distribution was narrower.

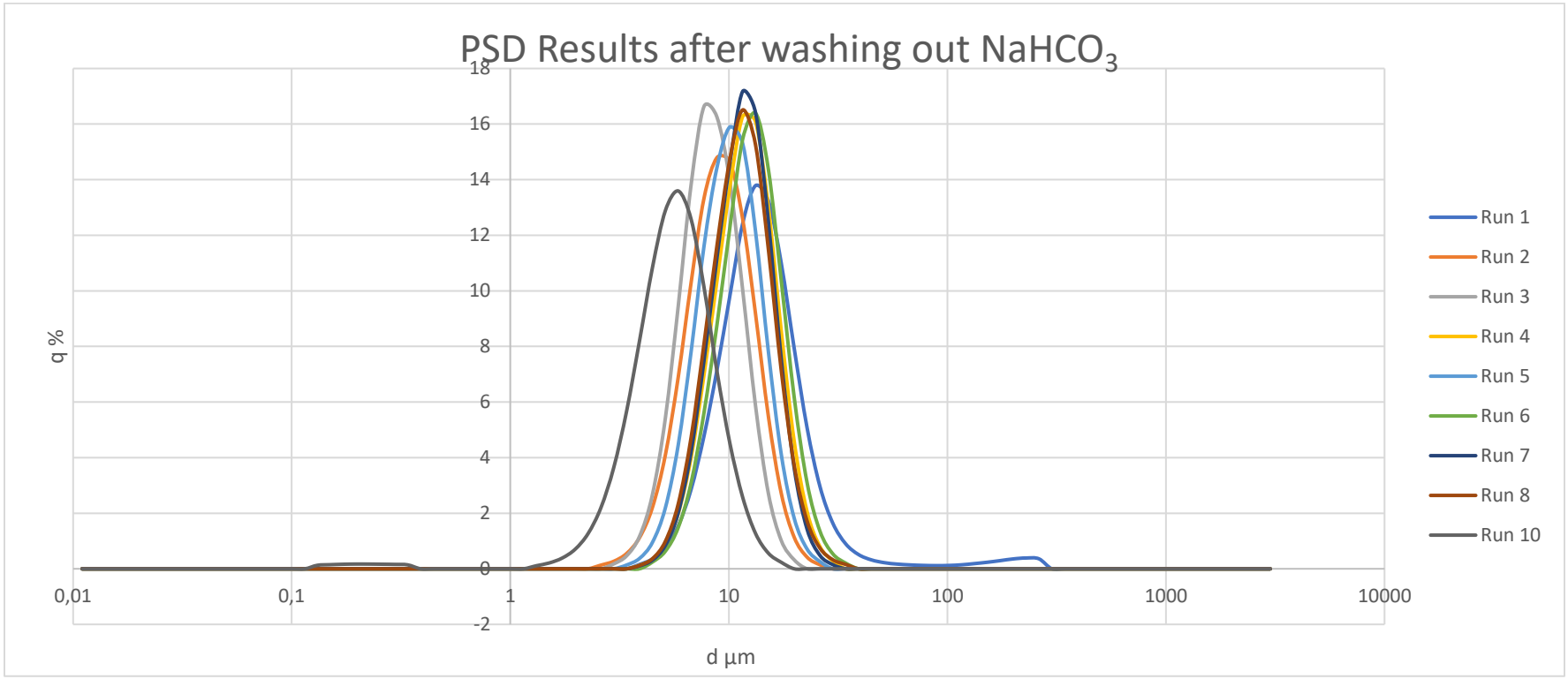

Figure 14 Graphical representation of PSD of the PCC after washing the NaHCO3 (system ii)

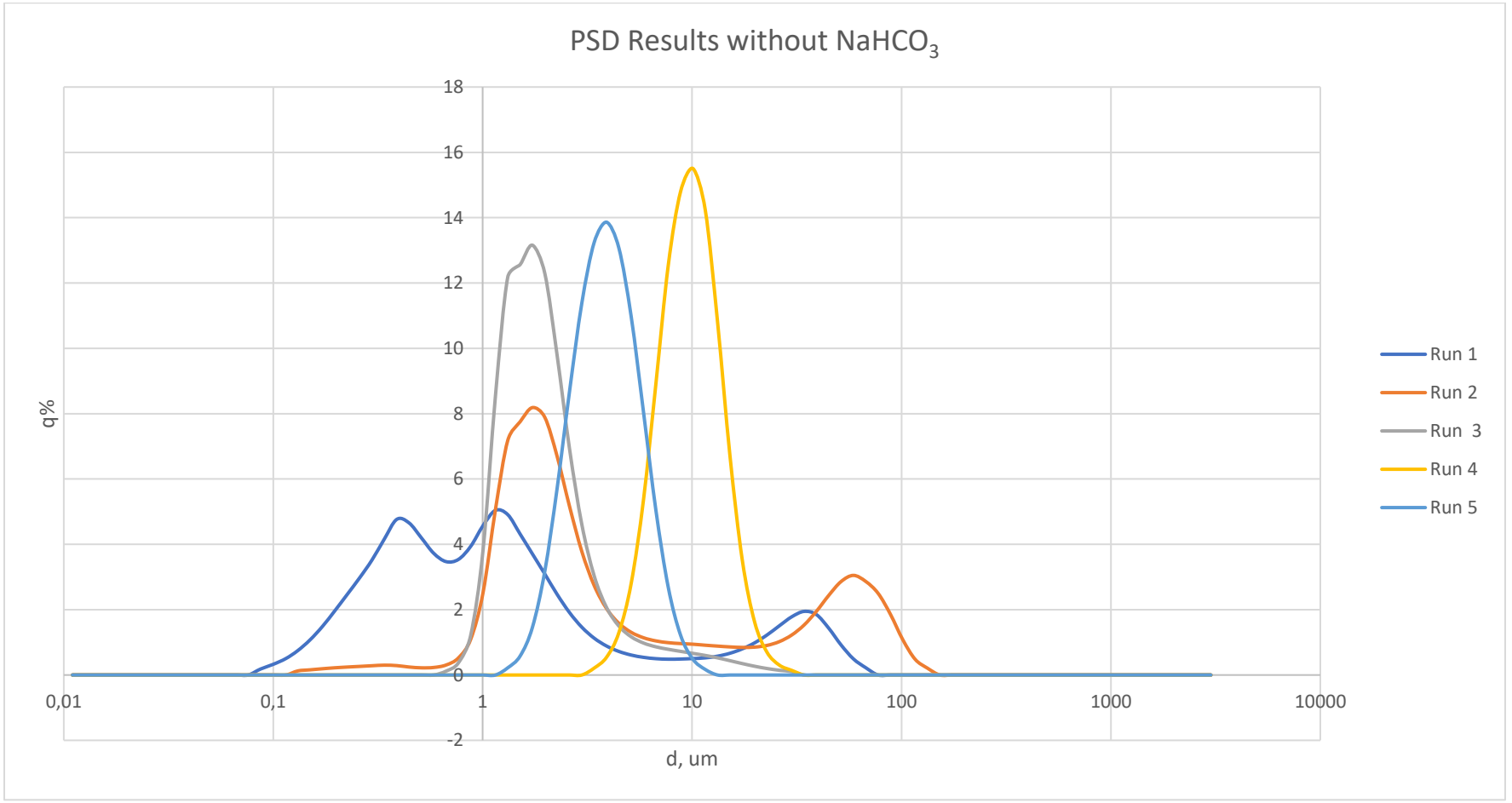

Figure 15 Graphical representation of PSD of the PCC (system i)

3.4.2 Morphology

The PCC products from both systems were dried and morphological analysis w carried out on the PCC. This was done using the Zeiss EVO MA15 (University of Tartu, Department of Geology).

From the analytical result, the morphology of the PCC obtained after the carbonation procedure in system (i) consisted mostly of vaterite spheres under these conditions: (L/S =5, 2 M NH_4COOCH_3), varying temperature and amount of CO_2 used.

The sizes are seen to be increasing with increase in temperature. Increasing operating temperature from 20->60°C at lower CO_2 concentrations (15% CO_2) changes the morphology - aragonite dumbbells, on average 5-7 µm in length and 2-3 µm wide, with occasional spherulites and larger clumps. Increasing operating temperature from 20->60°C at higher CO_2 concentrations (100% CO_2) produces 1 - 4 µm asymmetric vaterite aggregates + finer undefined particles that may be partly aragonite.

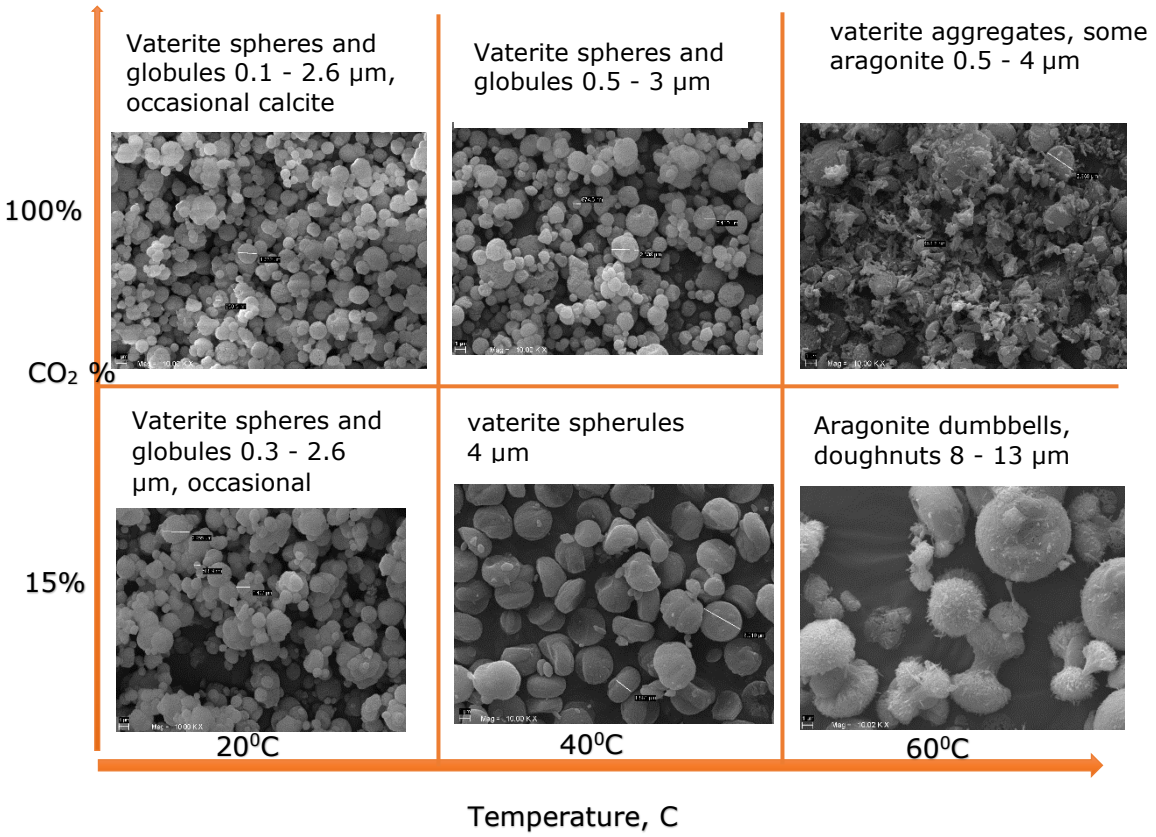

Figure 16 SEM images of the product PCC of system (i) without the addition of $NaHCO_3$

SEM images from the University of Tartu can be seen in Figure 16. The morphology for system (ii) were not reported because they were not yet available before the submission of this work.

3.4.3 Purity

The purity of the product PCC from system (ii) with the addition of $NaHCO_3$ was analyzed and the results showed that pure PCC was obtained from this experiment as we had six results showing purity ranging from 97 – 99% as seen in table 14.

The result with 92% purity may be due to impurities from the $NaHCO_3$ additive and this could be made purer with further washing.

ICP analysis for i system indicated that product purity was 98 - 99%, depending on ash type. The main impurity is anhydrite/gypsum (0.4 – 1.8%).

Table 15 Carbonisation procedure results

	Li	B	Na	Mg	Al	S	K	Ti	V	Cr	Mn	Fe	Co	Ni	Cu	Zn	As	Se	Sr	Ba	Tl	Pb
	mg/kg	mg/kg	mg/kg	mg/kg	mg/kg	mg/kg	mg/kg	mg/kg	mg/kg	mg/kg	mg/kg	mg/kg	mg/kg	mg/kg	mg/kg	mg/kg	mg/kg	mg/kg	mg/kg	mg/kg	mg/kg	mg/kg
ARAcarb1	0,48	7,97	42,77	249,52	2,51	**1673,51**	27,48	0,06	2,18	0,28	0,47	4,53	0,06	0,42	1,91	9,22	0,50	0,14	42,26	6,38	0,18	0,08
ARAcarb7	0,17	70,57	23,32	212,37	2,87	**3833,06**	182,96	0,06	17,36	0,61	0,85	3,39	0,03	< LOD	0,21	1,45	1,44	0,28	139,06	23,22	0,20	0,05
ARAcarb7x	0,12	67,59	20,39	221,83	3,06	**3730,89**	195,49	0,08	18,24	0,64	0,87	3,72	0,03	< LOD	0,19	1,37	1,44	0,23	142,23	23,26	0,19	0,05
ARAcarb8	0,21	11,61	24,05	325,96	3,29	**2399,48**	25,27	0,10	3,07	0,55	0,57	19,58	0,07	0,30	1,53	7,77	0,45	0,09	41,85	6,44	0,08	0,11
ARAcarb9	0,26	46,51	26,18	320,78	2,36	**3425,11**	9,11	0,09	8,53	0,72	1,18	3,98	0,05	0,23	0,38	3,56	1,02	0,16	29,13	4,52	0,12	0,07
ARAcarb1.1	0,27	7,46	37,44	130,25	< LOD	**1461,16**	37,29	< LOD	1,63	0,57	< LOD	2,95	0,09	0,36	2,32	7,15	0,34	0,12	25,90	3,04	0,19	0,03
ARAcarb1.3	0,27	5,08	40,75	140,18	1,15	**1468,68**	35,33	< LOD	1,47	0,43	< LOD	2,93	0,07	0,64	3,08	7,22	0,29	0,09	30,54	3,71	0,22	0,04
ARAcarb1.10	0,24	9,13	34,35	168,10	0,74	**1576,46**	28,84	0,07	1,81	0,53	< LOD	3,42	0,08	0,31	1,82	6,03	0,33	0,09	30,61	3,10	0,17	0,02
ARAcarb3.1	0,50	1,07	62,11	69,03	5,38	**971,12**	58,95	< LOD	0,08	1,20	0,23	6,09	0,07	1,10	4,69	19,70	0,07	0,03	41,66	6,57	0,17	0,09

	Product purity, %	**$CaSO_4$, %**	Others, % (calculated as carbonates)
ARAcarb1	99,19	0,71	0,10
ARAcarb7	98,20	1,63	0,17
ARAcarb7x	98,24	1,59	0,18
ARAcarb8	98,86	1,02	0,12
ARAcarb9	98,43	1,46	0,11
ARAcarb1.1	99,31	0,62	0,06
ARAcarb1.3	99,31	0,62	0,07
ARAcarb1.10	99,26	0,67	0,07
ARAcarb3.1	99,52	0,41	0,07

4. Process model and economics

Equilibrium composition of leaching and precipitation process simulations in this work were carried using the ASPEN PLUS V.10 software package designed for various tasks of model building such as simulation, parameter estimation, sensitivity analysis and optimization. The software consists of a GLOBAL and HENRY'S COMPONENT library of objective functions, solvers and optimizer linked to model problem-dependent routines and the objective function. The Aspen Plus RGibbs reactor model uses a Gibbs free energy minimization technique to determine the composition of each phase. This was employed to predict the equilibrium composition of both the Ca extraction and carbonisation systems.

Figure 17 illustrates the OSA to PCC process model that was used for the experiment.

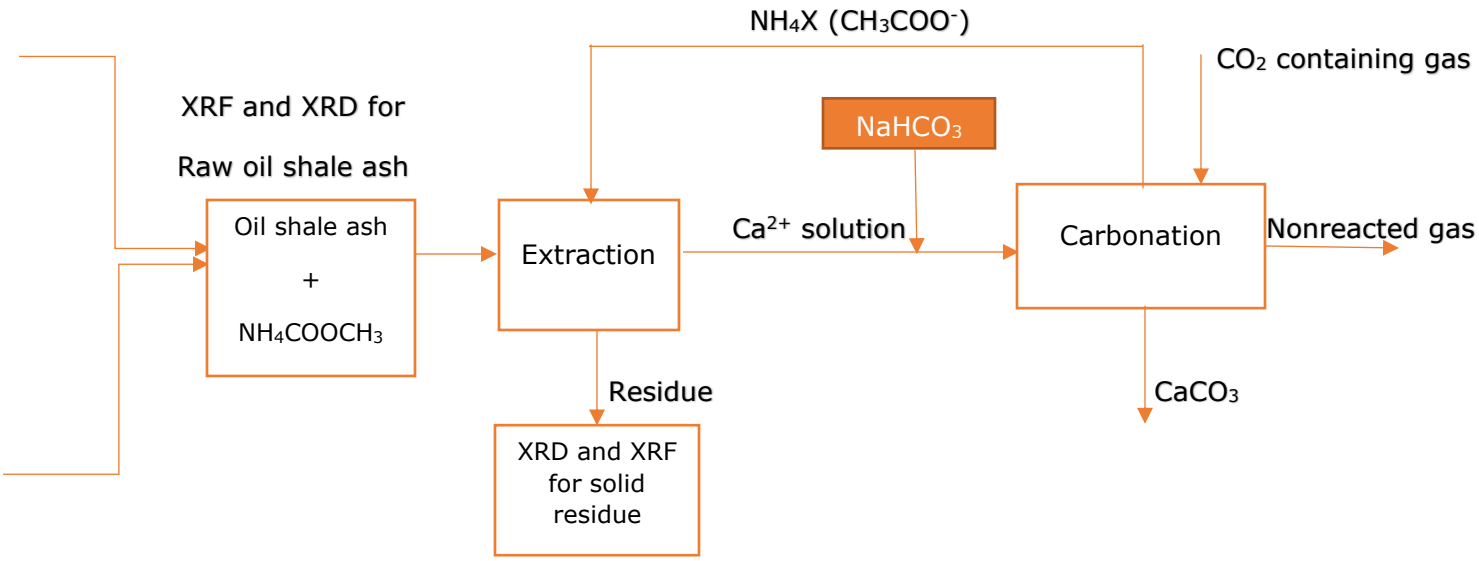

Figure 17 Process model for OSA to PCC production

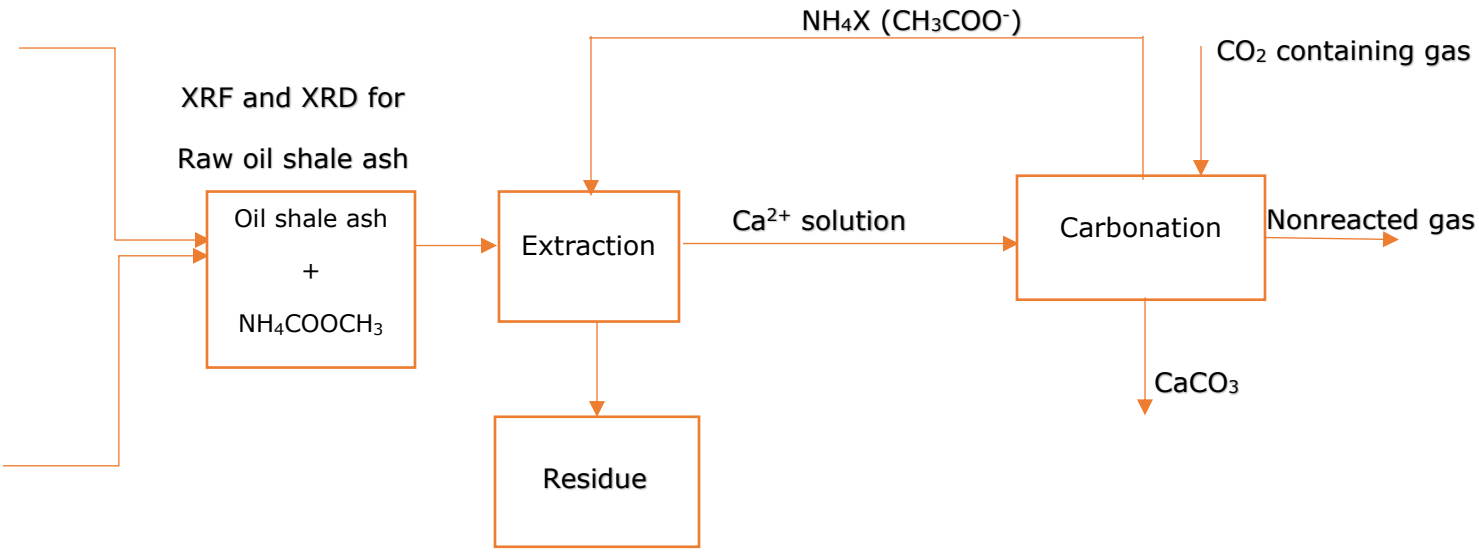

Figure 18 Process model for OSA to PCC production without the addition of $NaHCO_3$

The RGibbs reactor was used to model the Ca extraction from OSA. The suspended result was channeled to the solid-liquid centrifuge (separator) where the Ca^{2+} solution was separated from the residue. $NaHCO_3$ was added to this Ca^{2+} rich solution and was channeled into another RGibbs reactor which stood as an inlet and outlet chamber for the CO_2 gas that was bubbled into the reactor. At the end of the reaction, the suspension containing PCC was drained out and then dried to separate the PCC from the solvent.

In figure 18, it was carried out the same process without the addition of $NaHCO_3$.

This simulation was done to analyse the equilibrium composition in the Ca^{2+} extraction stage and the carbonation stage. The results derived from the analysis of the solid and liquid phase compositions are illustrated in tables 16 - 18.

Table 16 Liquid phase composition (Model result)

Composition	Solvent in	Ca-solution (extract)	Electroneutrality (extract) mol/L		Solvent out (Filt)	Electroneutrality (Filt) mol/L	
	mol/L	mol/L	Cations	Anions	mol/L	Cations	Anions
CO_2	0	7.61E-13			3.42E-08		
N_2	0	2.33E-13			6.78E-09		
NH_3	0	1.88565			0.631821		
H_20	42.61421	41.25566			41.51692		
H^+	0	5.71E-11			7.22E-09		
OH^-	0	0.00468			4.89E-05		
CO_3^{2-}	0	1.82E-07		3.64E-07	7.78E-07		1.556E-06
HCO_3^-	0	1.3E-08		1.3E-08	1.11E-05		1.11E-05
H_3O^+	0	4.69E-11			6.1E-09		
Ca^{2+}	0	0.944895	1.88979		0.324386	0.648772	
$CaOH^+$	0	0.018551			5.5E-05		
Na^+	0	0			0		
NH_4^+	2	0.032367	0.032367		1.312961	1.312961	
$HSiO_4^{3-}$	0	1.84E-07			8.69E-07		
SiO_4^{4-}	0	7.21E-10			2.77E-13		
$H_3SiO_4^-$	0	1.26E-07			5.97E-05		
$HSiO_3^-$	0	5.33E-08			2.47E-05		
SO_4^{2-}	0	1.32E-10			8.04E-09		
Mg^{2+}	0	0.000207			0.002147		
K^+	0	0			0		
Fe^{3+}	0	0			0		
CH_3COO^-	2	1.894328		1.894328	1.916495		1.916495
SO_3^{2-}	0	1.12E-12			1.02E-12		
HSO_3^-	0	0			2.72E-14		
S_2O3^{2-}	0	0.021001		0.042002	0.024653		0.049306
			1.9222	1.9363		1.9617	1.9658

Table 17 Liquid phase composition of Auvere (FA+Gen experimental result)

Composition	Ca-solution (extract)	Electroneutrality (extract) mol/L		Solvent out (Filt)	Electroneutrality (Filt) mol/L	
	mol/L	Cations	Anions	mol/L	Cations	Anions
F^-	1.316482		1.316482	0.011585		0.011585
SO_4^{2-}	11.45833		22.91667	7.291667		14.58333
Cl^-	7.203389		7.203389	12.42938		12.42938
SO_3^{2-}	7.525		15.05			69.77778
Ca^{2+}	548.9843	1097.9688		157.2091	314.4183	
Mg^{2+}	4.732510	9.465022		2.633744	5.26749	
K^+	5.882352	5.882352		8.184143	8.184143	
$S_2O_3^{2-}$	10.70186		21.403727			30
Fe^{2+}	0.001432	0.0028651		0.001432	0.002865	
Ba^{2+}	0.000728	0.0014564		0.004369	0.008738	
CH_3COO^-	2033.8983		2033.8983	440.678		440.678
OH^-			0.0002238	1.09E-06		1.09E-06
NH_4^+	1111.1111	1111.1111		193.3333	193.3333	
H^+	4,467E-11	4,467E-11		3,16E-05	3,16E-05	
		2224,4316	2101,7887		521,2149	567,48

Table 18 Solid phase composition (XRD) (model results)

Composition	Initial Ash (Auvere FA + Gen)	Residue	PCC
	%	%	%
LIME	**24.40**	**0**	**0**
PORTLANDITE	**0.00**	5.057	0
C2S, beta	**8.00**	**0.589**	**0**
QUARTZ	**12.2**	**11.228**	**0.004**
CALCITE	13.2	17.165	99.996
ANHYDRITE	9.7	8.749	0
PERICLASE	3.70	3.065	0
HEMATITE	4.30	3.958	0
K-FELDSPAR	10.6	9.756	0
GYPSUM	0.00	0.000	0
AKERMANITE	2.20	6.327	0
$MgSiO_3$	0.00	0.000	0
Muscovite	7.80	7.179	0
WOLLASTONITE	0.00	1.267	0
DOLOMITE	1.10	0.000	0
MERWINITE	2.80	2.062	0

The model predicted quite well the changes in solid and liquid phases as well as precipitation of CaCO3. From the experimental result derived compared to the model result, the liquid phase composition is slightly different as shown in tables 16 and 17, there was Ba^{+} and F^{-} ions present in the experimental result but absent in the model result. The highlighted compositions are the main liquids and solids that reacts together for the formation of PCC. The electroneutrality of the filtrate resulting from the model simulation was also measured and it showed the filtrate to be electrically neutral. When the electroneutrality of the experimental filtrate was measured as seen in table 16, it was not electrically neutral. There was a major difference between the electroneutrality of the model sample and that of the experimental sample.

Modelling results indicated that 73575.5 kg PCC can be produced from 176000 kg Auvere ash (0.42 kg/kg) using 92511.78 kg fresh solvent (0.52 kg/kg 2M NH_4COOCH_3 solution or 0.09 kg/kg NH_4COOCH_3).

.

4.1 Economic evaluation

During the experimental procedure, the materials and the parameters used to produce the PCC were analysed. Also, the cost incurred while running this process was consider and these accountabilities will give room to further improve future projects if necessary.

4.1.1 Operating cost

The variable costs that were considered are in relation to the types of samples, the electricity consumed, the equipment and apparatus, flue gas etc. used in producing the PCC. This cost varies depending on the quantities of materials needed and if they can be found in close by locations or have to be imported.

Also, the process design is another form of cost that can be incurred because if there are no previous studies on the types of reactors or process conditions to be used, then it needs to be determined by trying out different reactors or equipment until a suitable one is found after which the final installation cost can be determined.

When all equipment and material costs have been determined, then the installation, labour and maintenance costs should also be put in place. All these costs are then calculated and added to the overall cost of carrying out the experiment at either the laboratory or pilot scale.

4.1.2 External effect evaluation

There are some major factors that come into play with carrying out this kind of experiment. These are environmental, social and tax factors.

For the environmental factor, protection of the atmosphere and ecosystem must be considered when deciding on the kind of fuel and electricity to be used and the combustion

procedure must be analysed. Ensuring that green sources for generation power are used gives the project a good chance of approval Sustainable development law makers.

Looking at the social aspect, the project should be a source of development to the locations where there are being operated. This can be a source of job creation for the inhabitants of the community or can boost the livelihood of the people living in such areas.

When taxes are paid according to the regulations of the country regarding a project for instance, due to CO_2 emissions, then the company gets approval in case they need to carry out other projects as they are considered trustworthy.

5. CONCLUSION

This thesis work focused mainly on the production of high-quality PCC from ash-NH_4COOCH_3 system with the addition of $NaHCO_3$ under varying conditions.

The results were achieved through the literature studies, modelling and experimental plans. The various effects the operating parameters had on the leaching, carbonation and product quality gave an insight on the favourable conditions for high-quality PCC production.

The main carbonation process parameters were temperature of 20-60C, CO_2 concentration (15-100%) and rotation speed (200-600 rpm) that influenced the morphology and particle size of the PCC produced in system (i). Mostly vaterite in size range of 1 – 4 µm PCC was produced under ambient temperature. Increasing operating temperature from 20->60^oC at lower CO_2 concentrations (15% CO_2) changes the morphology - aragonite dumbbells, on average 5-7 µm in length and 2-3 µm wide, with occasional spherulites and larger clumps. Increasing operating temperature from 20->60^oC at higher CO_2 concentrations (100% CO_2) produces 1-4 µm asymmetric vaterite aggregates + finer undefined particles that may be partly aragonite. ICP analysis indicated that product purity was 98 - 99%. The main impurity is anhydrite/gypsum (0.4 – 1.8%).

The addition of $NaHCO_3$ enhanced and increased the particle sizes in system (ii) (5 - 13 µm). Using additive in given concentrations (0.2 – 0.7 mol/L) proved to be not effective, because in addition to PCC also the additive precipitated and had to be washed using multiple washing cycles.

The simulation model on Aspen Plus platform can be used to determine the oil shale ash leaching and carbonation results in comparison with the experimental results. It can also be used to predict the liquid and solid phase compositions in the ash-NH_4COOCH_3 system. Modelling results indicated that 73575.5 kg PCC can be produced from 176000 kg Auvere ash (0.42 kg/kg) using 92511.78 kg fresh solvent (0.52 kg/kg 2M NH_4COOCH_3 solution or 0.09 kg/kg NH_4COOCH_3).

The results of this work are up for further studies on optimization of Ca extraction and carbonisation process as well as kinetics.

SUMMARY

In the year 2020 in Estonia, approximately 6.4 million tons of oil shale got burned for power and energy generation. The ashes are mainly deposited on land fields, and only a small amount is utilized. Also, the combustion of oil shale generates CO_2 emissions which is the main precursor of climate change. Hence, measures must be taken to reduce the pollution caused by oil shale industry.

In this thesis work, oil shale ash from Auvere power plant was used to produce precipitated calcium carbonate. This was seen as a viable means of reducing oil shale ash deposition on ash fields as well as CO2 emissions into atmosphere as they can be channeled into making useful industrial products.

The experimental procedure consisted of the Ca-extraction and the carbonation stages. Two different sets experiments were studied – with and without the additive ($NaHCO_3$) in the system of OSA-NH_4COOCH_3 solution– CO_2 containing model gas.

The main parameters influencing the product (PCC) properties were temperature (20-60C), CO_2 concentration (15-100%) and rotation speed (200-600 rpm). Mostly vaterite of in size range of 1 – 4 μm PCC was produced under ambient temperature. Increasing operating temperature from 20->60^oC at lower CO_2 concentrations (15% CO_2) changes the morphology to aragonite dumbbells, on average 5-7 μm in length and 2-3 μm wide, with occasional spherulites and larger clumps. Increasing operating temperature from 20->60^oC at higher CO_2 concentrations (100% CO_2) produces 1-4 μm asymmetric vaterite aggregates + finer undefined particles that may be partly aragonite. ICP analysis indicated that product purity was 98 - 99%. The main impurity is anhydrite/gypsum (0.4 – 1.8%).

Model simulation using Aspen Plus platform was also used to predict the dissolution behavior in the solid and liquid phases, and these were compared with the experimental results obtained. Modelling results indicated that 73575.5 kg PCC can be produced from 176000 kg Auvere ash (0.42 kg/kg) using 92511.78 kg fresh solvent (0.52 kg/kg 2M NH_4COOCH_3 solution or 0.09 kg/kg NH_4COOCH_3).

The thesis focused on producing high-quality PCC under some operating conditions and it was observed that there is still room for further studies to improve the leaching, carbonation, and model simulation for high grade PCC production viable for industrial usage.

REFERENCES

[1] "Management Report Financial Statements."

[2] T. Pihu, A. Konist, E. Puura, M. Liira, and K. Kirsimäe, "PROPERTIES AND ENVIRONMENTAL IMPACT OF OIL SHALE ASH LANDFILLS," *Oil Shale*, vol. 36, no. 2, pp. 257–270, 2019, doi: 10.3176/oil.2019.2.01.

[3] "Ragn-Sells invests in resource saving carbon capture and utilisation project in Estonia | Ragn-Sells Group." https://www.mynewsdesk.com/ragnsells/pressreleases/ragn-sells-invests-in-resource-saving-carbon-capture-and-utilisation-project-in-estonia-3007479 (accessed Apr. 18, 2021).

[4] "OSAMAT-Management of environmentaly sound recycling of oil-shale ashes into road construction products. Demonstration in Estonia."

[5] O. Velts, M. Kindsigo, M. Uibu, J. Kallas, and R. Kuusik, "CO2 mineralisation: Production of CaCO3-type material in a continuous flow disintegrator-reactor," *Energy Procedia*, vol. 63, no. December, pp. 5904–5911, 2014, doi: 10.1016/j.egypro.2014.11.625.

[6] "BCCF Calcium Carbonate | Uses of calcium carbonate from Middles Ages to the Industrial Revolution." http://www.calcium-carbonate.org.uk/calcium-carbonate/caco3-history2.asp (accessed Apr. 18, 2021).

[7] W. Zappa, "Pilot-scale Experimental Work on the Production of Precipitated Calcium Carbonate (PCC) from Steel Slag for CO 2 Fixation requirements for the degree of Department of Energy Technology," no. August, 2014.

[8] "What is main differences between precipitated calcium carbonate/PCC and ground calcium carbonate/GCC?" http://www.wsdchemical.com/technical-support/diffrence-of-pcc-and-gcc.html (accessed Apr. 25, 2021).

[9] R. Salomão, L. M. M. Costa, and G. M. de Olyveira, "Precipitated Calcium Carbonate Nano-Microparticles: Applications in Drug Delivery," *Adv. Tissue Eng. Regen. Med. Open Access*, vol. 3, no. 2, Nov. 2017, doi: 10.15406/atroa.2017.03.00059.

[10] P. Stratton, "An Overview of the North American Calcium Carbonate Market," no. October, p. 43, 2012.

[11] H. P. Mattila and R. Zevenhoven, "Production of Precipitated Calcium Carbonate from Steel Converter Slag and Other Calcium-Containing Industrial Wastes and Residues," in *Advances in Inorganic Chemistry*, vol. 66, Academic Press Inc., 2014, pp. 347–384.

[12] "Pigment Coating and Surface Sizing of Paper, 2nd Edition." https://imisrise.tappi.org/TAPPI/Products/02/FIN/0202FIN11-2.aspx (accessed Apr. 25, 2021).

[13] "Calcium, carbonate hydroxy aluminum complexes - Registration Dossier - ECHA." https://poisoncentres.echa.europa.eu/web/guest/registration-dossier/-/registered-dossier/8086/7/5/1 (accessed Apr. 25, 2021).

[14] S. Teir, S. Eloneva, and R. Zevenhoven, "Production of precipitated calcium carbonate from calcium silicates and carbon dioxide," *Energy Convers. Manag.*, vol. 46, no. 18–19, pp. 2954–2979, Nov. 2005, doi: 10.1016/j.enconman.2005.02.009.

[15] R. Zevenhoven, "Metals production, CO2 mineralization and LCA," *Metals (Basel).*, vol. 10, no. 3, 2020, doi: 10.3390/met10030342.

[16] S. El-Sherbiny, F. A. Morsy, A. M. Atta, and S. A. Ahmed, "Preparation of Water Based Polymeric Binders for Paper Surface Coating," *J. Surf. Eng. Mater. Adv. Technol.*, vol. 04, no. 03, pp. 140–154, 2014, doi: 10.4236/jsemat.2014.43018.

[17] "Schematic-diagram-of-the-lime-soda-process-5." .

[18] N. Czaplicka and D. Konopacka-Łyskawa, "Utilization of gaseous carbon dioxide and industrial ca-rich waste for calcium carbonate precipitation: A review," *Energies*, vol. 13, no. 23, pp. 7–14, 2020, doi: 10.3390/en13236239.

[19] Y. Yanagisawa, "A new CO2 disposal process via artificial weathering of calcium silicate accelerated by acetic acid," *Energy*, vol. 26, no. 4, pp. 341–354, Apr. 2001, doi: 10.1016/S0360-5442(01)00005-6.

[20] R. Zevenhoven, S. Eloneva, and S. Teir, "Chemical fixation of CO2 in carbonates: Routes to valuable products and long-term storage," *Catal. Today*, vol. 115, no. 1–4, pp. 73–79, Jun. 2006, doi: 10.1016/j.cattod.2006.02.020.

[21] S. Kodama, T. Nishimoto, N. Yamamoto, K. Yogo, and K. Yamada, "Development of a new pH-swing CO2 mineralization process with a recyclable reaction solution," *Energy*, vol. 33, no. 5, pp. 776–784, May 2008, doi: 10.1016/j.energy.2008.01.005.

[22] "Integrated Pollution Prevention and Control Reference Document on Best Available

Techniques for the Manufacture of Large Volume Inorganic Chemicals-Solids and Others industry," 2007. Accessed: Apr. 26, 2021. [Online]. Available: http://eippcb.jrc.es.

[23] "Pulp and Paper Industry - 1st Edition." https://www.elsevier.com/books/pulp-and-paper-industry/bajpai/978-0-12-803408-8 (accessed Apr. 26, 2021).

[24] "Worldwide Calcium Carbonate Industry to 2025 - Increasing Demand from the Paper Industry is Driving Growth." https://www.globenewswire.com/news-release/2021/01/14/2158922/0/en/Worldwide-Calcium-Carbonate-Industry-to-2025-Increasing-Demand-from-the-Paper-Industry-is-Driving-Growth.html (accessed Apr. 26, 2021).

[25] "Calcium Carbonate Market Worth $7.75 Billion By 2025 | CAGR: 7.4% – Site Title." https://trendinresearchreport.wordpress.com/2020/05/15/global-calcium-carbonate-market-outlook/ (accessed Apr. 26, 2021).

[26] C. M. Sundermann, "Production of Calcium Carbonate from Steelmaking Slag and Captured CO2- Optimisation of the Carbonation Process and Product Quality," p. 94, 2016.

[27] G. Wolf and C. Günther, "THERMOPHYSICAL INVESTIGATIONS OF THE POLYMORPHOUS PHASES OF CALCIUM CARBONATE," 2001.

[28] M. M. Tlili, M. Ben Amor, C. Gabrielli, S. Joiret, G. Maurin, and P. Rousseau, "Characterization of CaCO 3 hydrates by micro-Raman spectroscopy," pp. 10–16, 2002.

[29] C. K. Chen and C. Y. Tai, "Competing effects of operating variables in the synthesis of CaCO3 particles using the reverse microemulsion technique," *Chem. Eng. Sci.*, vol. 65, no. 16, pp. 4761–4770, Aug. 2010, doi: 10.1016/j.ces.2010.05.019.

[30] M. G. Lioliou, C. A. Paraskeva, P. G. Koutsoukos, and A. C. Payatakes, "Heterogeneous nucleation and growth of calcium carbonate on calcite and quartz," *J. Colloid Interface Sci.*, vol. 308, no. 2, pp. 421–428, Apr. 2007, doi: 10.1016/j.jcis.2006.12.045.

[31] O. Velts, *Oil shale Ash as a Source of Calcium Carbonate: Process Feasibility, Mechanism and Modeling.*, vol. Doctor of. 2011.

[32] M. Kitamura, "Crystallization and transformation mechanism of calcium carbonate polymorphs and the effect of magnesium ion," *J. Colloid Interface Sci.*, vol. 236, no. 2, pp. 318–327, Apr. 2001, doi: 10.1006/jcis.2000.7398.

[33] R. Louis Thatcher, "United States Patent (19)," 2000.

[34] E. Dalas, J. Kallitsis, and P. G. Koutsoukos, "The crystallization of calcium carbonate on polymeric substrates," *J. Cryst. Growth*, vol. 89, no. 2–3, pp. 287–294, Jun. 1988, doi: 10.1016/0022-0248(88)90412-5.

[35] H. Konno, Y. Nanri, and M. Kitamura, "Crystallization of aragonite in the causticizing reaction," *Powder Technol.*, vol. 123, no. 1, pp. 33–39, Feb. 2002, doi: 10.1016/S0032-5910(01)00424-7.

[36] N. Technology, "Nano Precipitated Calcium Carbonate (NPCC) for Plastic Industry.pdf." pp. 5–6, 2015.

[37] O. Velts, M. Uibu, I. Rudjak, J. Kallas, and R. Kuusik, "Utilization of oil shale ash to prepare PCC: Leachibility dynamics and equilibrium in the ash-water system," in *Energy Procedia*, Feb. 2009, vol. 1, no. 1, pp. 4843–4850, doi: 10.1016/j.egypro.2009.02.312.

[38] O. Velts, M. Uibu, J. Kallas, and R. Kuusik, "Waste oil shale ash as a novel source of calcium for precipitated calcium carbonate: Carbonation mechanism, modeling, and product characterization," *J. Hazard. Mater.*, vol. 195, pp. 139–146, Nov. 2011, doi: 10.1016/j.jhazmat.2011.08.019.

[39] O. Velts, M. Kindsigo, M. Uibu, J. Kallas, and R. Kuusik, "CO2 mineralisation: Production of CaCO3-type material in a continuous flow disintegrator-reactor," in *Energy Procedia*, 2014, vol. 63, pp. 5904–5911, doi: 10.1016/j.egypro.2014.11.625.

[40] J. A. Dirksen and T. A. Ring, "Fundamentals of crystallization: Kinetic effects on particle size distributions and morphology," *Chemical Engineering Science*, vol. 46, no. 10. Pergamon, pp. 2389–2427, Jan. 01, 1991, doi: 10.1016/0009-2509(91)80035-W.

[41] A. E. Al-Rawajfeh, "Factors influencing CaCO3 scale precipitation and CO2-H2O system in flowing water in natural water piping system," *Desalin. Water Treat.*, vol. 12, no. 1–3, pp. 337–343, 2009, doi: 10.5004/dwt.2009.969.

[42] D. Gómez-Díaz, J. M. Navaza, and B. Sanjurjo, "Analysis of mass transfer in the precipitation process of calcium carbonate using a gas/liquid reaction," *Chem. Eng. J.*, vol. 116, no. 3, pp. 203–209, Mar. 2006, doi: 10.1016/j.cej.2005.12.004.

[43] V. A. Juvekar and M. M. Sharma, "Absorption of CO2 in a suspension of lime," *Chem. Eng. Sci.*, vol. 28, no. 3, pp. 825–837, Mar. 1973, doi: 10.1016/0009-2509(77)80017-1.

[44] B. Cheng, M. Lei, J. Yu, and X. Zhao, "Preparation of monodispersed cubic calcium

carbonate particles via precipitation reaction," *Mater. Lett.*, vol. 58, no. 10, pp. 1565–1570, Apr. 2004, doi: 10.1016/j.matlet.2003.10.027.

[45] J. Hostomsky and A. G. Jones, "Calcium carbonate crystallization, agglomeration and form during continuous precipitation from solution," *J. Phys. D. Appl. Phys.*, vol. 24, no. 2, pp. 165–170, Feb. 1991, doi: 10.1088/0022-3727/24/2/012.

[46] M. Kitamura, H. Konno, A. Yasui, and H. Masuoka, "Controlling factors and mechanism of reactive crystallization of calcium carbonate polymorphs from calcium hydroxide suspensions," *J. Cryst. Growth*, vol. 236, no. 1–3, pp. 323–332, Mar. 2002, doi: 10.1016/S0022-0248(01)02082-6.

[47] H. P. Mattila, I. Grigaliu-naite, and R. Zevenhoven, "Chemical kinetics modeling and process parameter sensitivity for precipitated calcium carbonate production from steelmaking slags," *Chem. Eng. J.*, vol. 192, pp. 77–89, Jun. 2012, doi: 10.1016/j.cej.2012.03.068.

[48] "Precipitated Calcium Carbonate (PCC)." https://projects.ncsu.edu/project/hubbepaperchem/PCC.htm (accessed Apr. 26, 2021).

[49] Y. Sun, M. S. Yao, J. P. Zhang, and G. Yang, "Indirect CO2 mineral sequestration by steelmaking slag with NH4Cl as leaching solution," *Chem. Eng. J.*, vol. 173, no. 2, pp. 437–445, Sep. 2011, doi: 10.1016/j.cej.2011.08.002.

[50] A. G. Jones, J. Hostomsky, and L. Zhou, "On the effect of liquid mixing rate on primary crystal size during the gas-liquid precipitation of calcium carbonate," *Chem. Eng. Sci.*, vol. 47, no. 13–14, pp. 3817–3824, Sep. 1992, doi: 10.1016/0009-2509(92)85102-H.

[51] M. M. Reddy and G. H. Nancollas, "The crystallization of calcium carbonate. I. Isotopic exchange and kinetics," *J. Colloid Interface Sci.*, vol. 36, no. 2, pp. 166–172, Jun. 1971, doi: 10.1016/0021-9797(71)90161-5.

[52] W. M. Jung, S. H. Kang, W. S. Kim, and C. K. Choi, "Particle morphology of calcium carbonate precipitated by gas-liquid reaction in a Couette-Taylor reactor," *Chem. Eng. Sci.*, vol. 55, no. 4, pp. 733–747, Feb. 2000, doi: 10.1016/S0009-2509(99)00395-4.

[53] C. Domingo, E. Loste, J. Gómez-Morales, J. García-Carmona, and J. Fraile, "Calcite precipitation by a high-pressure CO2 carbonation route," *J. Supercrit. Fluids*, vol. 36, no. 3, pp. 202–215, Jan. 2006, doi: 10.1016/j.supflu.2005.06.006.

[54] A. M. López-Periago, R. Pacciani, C. García-González, L. F. Vega, and C. Domingo, "A breakthrough technique for the preparation of high-yield precipitated calcium carbonate," *J. Supercrit. Fluids*, vol. 52, no. 3, pp. 298–305, Apr. 2010, doi: 10.1016/j.supflu.2009.11.014.

[55] M. Ukrainczyk, J. Kontrec, V. Babić-Ivančić, L. Brečević, and D. Kralj, "Experimental design approach to calcium carbonate precipitation in a semicontinuous process," *Powder Technol.*, vol. 171, no. 3, pp. 192–199, Feb. 2007, doi: 10.1016/j.powtec.2006.10.046.

[56] E. Altay, T. Shahwan, and M. Tanoğlu, "Morphosynthesis of CaCO3 at different reaction temperatures and the effects of PDDA, CTAB, and EDTA on the particle morphology and polymorph stability," *Powder Technol.*, vol. 178, no. 3, pp. 194–202, Sep. 2007, doi: 10.1016/j.powtec.2007.05.004.

[57] G. Li, Z. Li, and H. Ma, "Preparation of aragonite by carbonization in CaCl2-NH 4Cl solution without any additives," in *Monatshefte fur Chemie*, Jan. 2014, vol. 145, no. 1, pp. 187–194, doi: 10.1007/s00706-013-0995-6.

[58] B. Feng, A. K. Yong, and H. An, "Effect of various factors on the particle size of calcium carbonate formed in a precipitation process," *Mater. Sci. Eng. A*, vol. 445–446, pp. 170–179, Feb. 2007, doi: 10.1016/j.msea.2006.09.010.

[59] R. Agnihotri, S. K. Mahuli, S. S. Chauk, and L. S. Fan, "Influence of surface modifiers on the structure of precipitated calcium carbonate," *Ind. Eng. Chem. Res.*, vol. 38, no. 6, pp. 2283–2291, 1999, doi: 10.1021/ie9900521.

[60] J. Franke and A. Mersmann, "The influence of the operational conditions on the precipitation process," *Chem. Eng. Sci.*, vol. 50, no. 11, pp. 1737–1753, Jun. 1995, doi: 10.1016/0009-2509(95)00028-4.

[61] J. H. Bang *et al.*, "Specific surface area and particle size of calcium carbonate precipitated by carbon dioxide microbubbles," *Chem. Eng. J.*, vol. 198–199, pp. 254–260, Aug. 2012, doi: 10.1016/j.cej.2012.05.081.

[62] B. Feng, A. K. Yong, and H. An, "Effect of various factors on the particle size of calcium carbonate formed in a precipitation process," *Mater. Sci. Eng. A*, vol. 445–446, pp. 170–179, Feb. 2007, doi: 10.1016/j.msea.2006.09.010.

[63] O. A. Jimoh, K. S. Ariffin, H. Bin Hussin, and A. E. Temitope, "Synthesis of precipitated

calcium carbonate: a review," *Carbonates and Evaporites*, vol. 33, no. 2, pp. 331–346, 2018, doi: 10.1007/s13146-017-0341-x.

[64] M. M. M. G. P. G. Mantilaka, D. G. G. P. Karunaratne, R. M. G. Rajapakse, and H. M. T. G. A. Pitawala, "Precipitated calcium carbonate/poly(methyl methacrylate) nanocomposite using dolomite: Synthesis, characterization and properties," *Powder Technol.*, vol. 235, pp. 628–632, Feb. 2013, doi: 10.1016/j.powtec.2012.10.048.

[65] J. Yu, M. Lei, B. Cheng, and X. Zhao, "Facile preparation of calcium carbonate particles with unusual morphologies by precipitation reaction," *J. Cryst. Growth*, vol. 261, no. 4, pp. 566–570, Feb. 2004, doi: 10.1016/j.jcrysgro.2003.09.035.

[66] J. Yu, H. Tang, B. Cheng, and X. Zhao, "Morphological control of calcium oxalate particles in the presence of poly-(styrene-alt-maleic acid)," *J. Solid State Chem.*, vol. 177, no. 10, pp. 3368–3374, Oct. 2004, doi: 10.1016/j.jssc.2004.06.007.

[67] L. Xiang, Y. Xiang, Z. G. Wang, and Y. Jin, "Influence of chemical additives on the formation of super-fine calcium carbonate," *Powder Technol.*, vol. 126, no. 2, pp. 129–133, Jul. 2002, doi: 10.1016/S0032-5910(02)00047-5.

[68] W. K. Park, S. J. Ko, S. W. Lee, K. H. Cho, J. W. Ahn, and C. Han, "Effects of magnesium chloride and organic additives on the synthesis of aragonite precipitated calcium carbonate," *J. Cryst. Growth*, vol. 310, no. 10, pp. 2593–2601, May 2008, doi: 10.1016/j.jcrysgro.2008.01.023.

[69] A. Szcześ, E. Chibowski, and L. Hołysz, "Influence of ionic surfactants on the properties of freshly precipitated calcium carbonate," *Colloids Surfaces A Physicochem. Eng. Asp.*, vol. 297, no. 1–3, pp. 14–18, Apr. 2007, doi: 10.1016/j.colsurfa.2006.10.014.

[70] H. Wei, Q. Shen, Y. Zhao, D. J. Wang, and D. F. Xu, "Influence of polyvinylpyrrolidone on the precipitation of calcium carbonate and on the transformation of vaterite to calcite," in *Journal of Crystal Growth*, Apr. 2003, vol. 250, no. 3–4, pp. 516–524, doi: 10.1016/S0022-0248(02)02484-3.

[71] W. Zhang, Y. Hu, L. Xi, Y. Zhang, H. Gu, and T. Zhang, "Preparation of Calcium Carbonate Superfine Powder by Calcium Carbide Residue," *Energy Procedia*, vol. 17, pp. 1635–1640, Jan. 2012, doi: 10.1016/j.egypro.2012.02.291.

[72] P. Liang, Y. Zhao, Q. Shen, D. Wang, and D. Xu, "The effect of carboxymethyl chitosan on the precipitation of calcium carbonate," *J. Cryst. Growth*, vol. 261, no. 4, pp. 571–

576, Feb. 2004, doi: 10.1016/j.jcrysgro.2003.03.001.

[73] H. Wei, Q. Shen, Y. Zhao, Y. Zhou, D. Wang, and D. Xu, "Effect of anionic surfactant-polymer complexes on the crystallization of calcium carbonate," *J. Cryst. Growth*, vol. 264, no. 1–3, pp. 424–429, Mar. 2004, doi: 10.1016/j.jcrysgro.2004.01.001.

[74] J. Kontrec, M. Ukrainczyk, V. Babić-Ivančić, and D. Kralj, "Synthesis of Calcium Carbonate by Semicontinuous Carbonation Method in the Presence of Dextrans," *Croat. Chem. Acta*, vol. 84, no. 1, pp. 25–32, May 2011, doi: 10.5562/cca1746.

[75] I. W. Kim, R. E. Robertson, and R. Zand, "Effects of some nonionic polymeric additives on the crystallization of calcium carbonate," *Cryst. Growth Des.*, vol. 5, no. 2, pp. 513–522, Mar. 2005, doi: 10.1021/cg049721q.

[76] D. Konopacka-Łyskawa, B. Kos¨cielska, and J. Karczewski, "Effect of some organic solvent-water mixtures composition on precipitated calcium carbonate in carbonation process," *J. Cryst. Growth*, vol. 418, pp. 25–31, May 2015, doi: 10.1016/j.jcrysgro.2015.02.019.

[77] "BET (Brunauer, Emmett and Teller) | Particle Analytical." https://particle.dk/methods-analytical-laboratory/surface-area-bet-2/ (accessed May 16, 2021).

[78] P. Kallaste, "Põlevkivi mineraalsete jäätmete leostustasakaalud mudelsüsteemides," 2015.

Appendix 1 Mass of PCC before and after washing in system(ii)

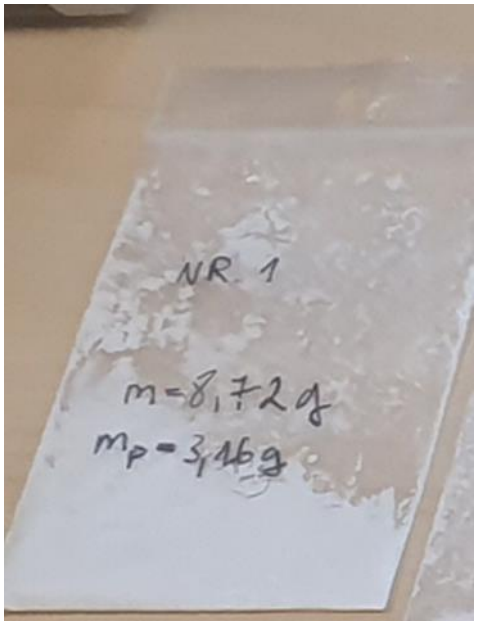

Before washing = 8.72g

After washing = 3.16g

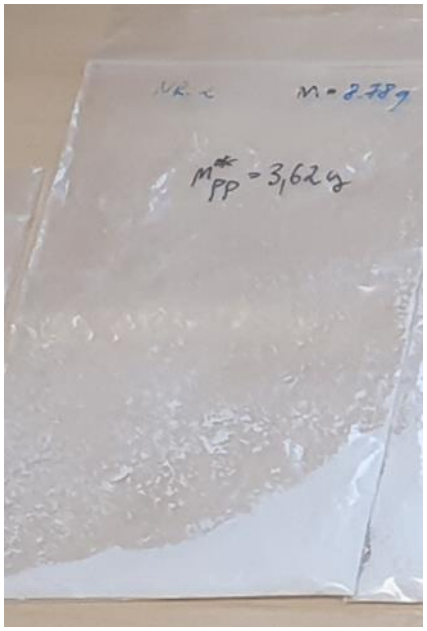

Before washing = 8.78g

After washing = 3.62g

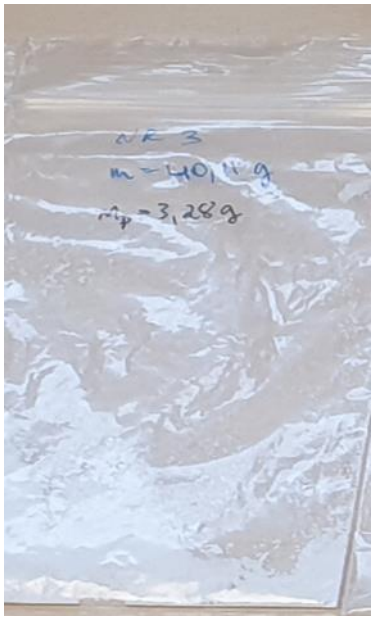

Before washing = 40.11g

After washing = 3.28g

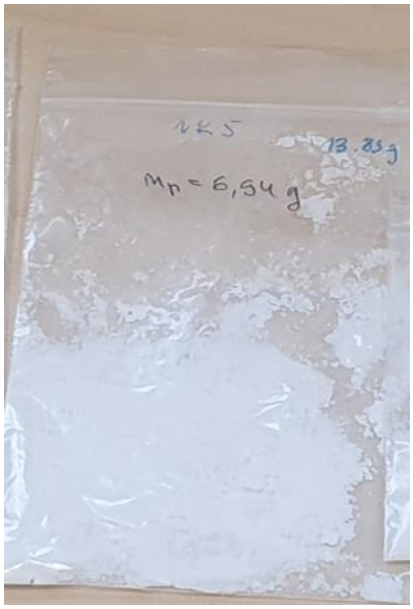

Before washing = 13.83g

After washing = 6.54g

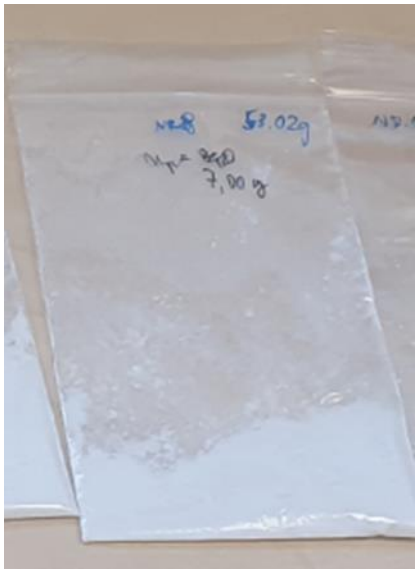

Before washing = 53.03g

After washing = 7.00g

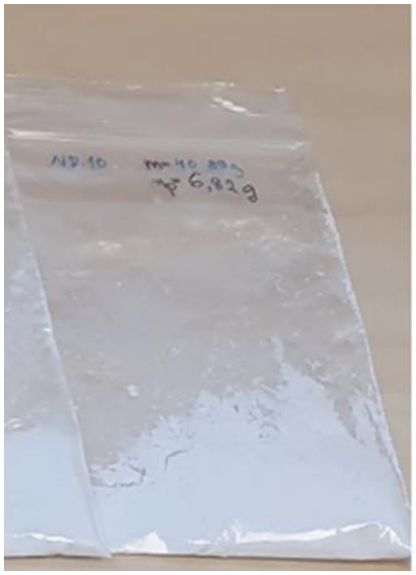

Before washing = 40.89g

After washing = 6.82g

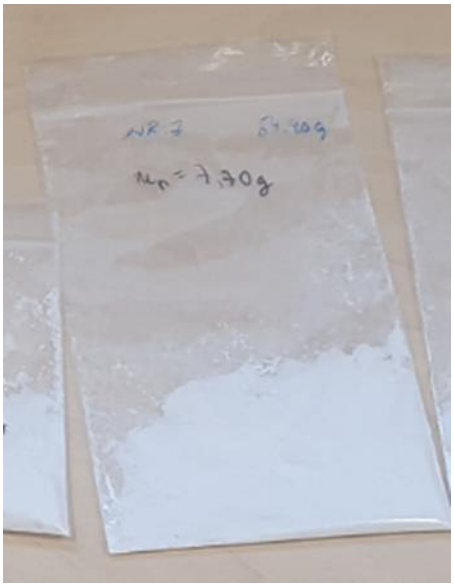

Before washing = 54.40g

After washing = 7.70g

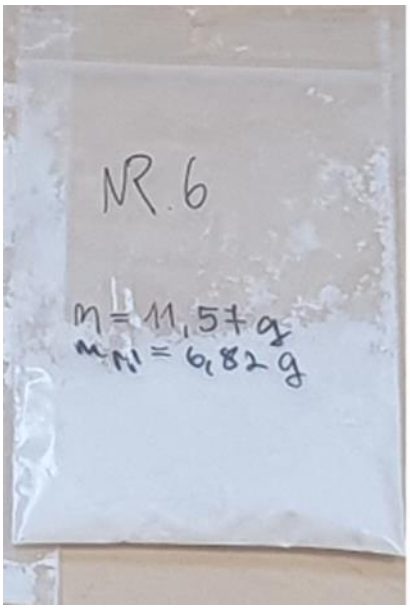

Before washing = 11.57g

After washing = 6.82g